ORIGINAL ARTICLE

lajss.org
Latin American Journal of Solids and Structures

www.lajss.org

Investigation of Seismic Response of S-Wave Incident Bedrock-Saturated Soil-Unsaturated Soil Site under Thermal Effect

Yongqin Ma[a], **Qiang Ma**[a,b*]

[a] School of Civil Engineering and Water Resources, Qinghai University, Xining 810016, China. Email: myq421086@163.com, maqiang0104@163.com
[b] Qinghai Provincial Key Laboratory of Energy-saving Building Materials and Engineering Safety, Xining 810016, China.

* Corresponding author

https://doi.org/10.1590/1679-7825/e8668

Abstract

Based on the theory of elastic wave propagation under thermal effects, this study develops a bedrock-saturated soil-unsaturated soil site model under S-wave incidence to investigate its seismic dynamic response. The analytical solution is derived using Helmholtz decomposition with appropriate boundary conditions. Numerical simulations systematically examine how thermal conductivity, saturation, and ground water level affect ground motion characteristics. Results demonstrate significant differences in displacement amplification factors between thermal and isothermal models. The thermal expansion coefficient and kelvin medium temperature substantially influence vertical displacement amplification, whereas thermal conductivity and heat flux phase delay show minimal effects. With increasing incident angle, horizontal displacement amplification decreases progressively while vertical amplification first increases then decreases. Higher ground water levels and saturation reduce horizontal displacement amplification but enhance vertical amplification.

Keywords

Thermal effect; Groundwater level; Bedrock-saturated soil-unsaturated soil site; Seismic ground motion; Plane S wave

Graphical Abstract

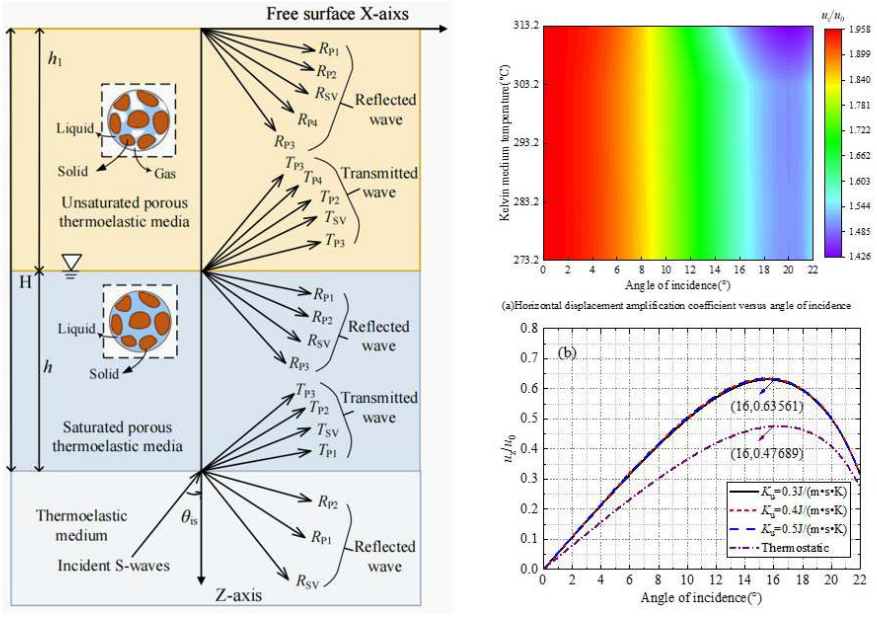

Received April 11, 2025. In revised form September 19, 2025. Accepted October 09, 2025. Available online October 10, 2025.
https://doi.org/10.1590/1679-7825/e8668

Latin American Journal of Solids and Structures. ISSN 1679-7825. Copyright © 2025. This is an Open Access article distributed under the terms of the Creative Commons Attribution license, which permits unrestricted use, distribution, and reproduction in any medium, provided the original work is properly cited

1 INTRODUCTION

The seismic ground motion response is significantly influenced by site conditions (FJ et al., 2015; Trifunac et al., 2016; Yu et al., 2021), often manifesting as amplification or attenuation of seismic waves. The properties of near-surface soils and hydrological conditions in epicentral regions are recognized as critical factors affecting seismic wave propagation characteristics (Wang et al., 2024; Lu et al., 2023). In recent years, temperature variations induced by global warming have exerted considerable impacts on the behavior of geomaterials (Ma, 2023), prompting increased attention to the coupled thermo-mechanical mechanisms through which site conditions influence seismic wave propagation (Zhang et al., 2024; Huang et al., 2022; Ba et al., 2017; Ba et al., 2020). However, existing research has predominantly focused on wave propagation under isothermal conditions, leaving the seismic performance of complex sites in non-isothermal environments inadequately explored.

The development of soil layer models has evolved from single-phase elastic media to saturated and unsaturated porous media. Biot (1956) first established the dynamic governing equations for saturated porous media. Based on this foundation, Wei et al. (2002), Cai et al. (2006), and Xu et al. (2009) subsequently developed wave propagation equations for unsaturated porous media. When waves encounter interfaces, reflection and transmission occur, exciting different types of waves and thereby influencing seismic motion characteristics (Ye et al., 2005; Jiang et al., 2017). Among various factors, degree of saturation (Yang, 2001; Li, 2002; Li et al., 2018; Xia et al., 2006; Zhao et al., 2012; Chen et al., 2013; Yao, 2023) and groundwater level (Wang, 2016; Hu, 2017) are crucial, as they not only alter wave propagation characteristics but also affect the energy carried by elastic waves. Subsequently, research has been extended to two-layer site models to investigate seismic response under oblique incident waves (Che, 2018; Hua et al., 2019; Dong, 2023). However, all the aforementioned studies are based on isothermal conditions and do not account for thermo-mechanical coupling effects.

Heat transfer within soil layers is an inherent physical phenomenon. With the increasing prominence of global warming, the impact of temperature variations on soil layers and engineering structures has attracted growing attention. Phenomena such as glacier melting and sea-level rise exacerbate thermal disturbances in geotechnical environments, posing serious challenges to the reliability of engineering construction. This has prompted in-depth research in fields such as thermodynamics and geotechnical engineering (Wen et al., 2021; Li, 2023; Liu, 2020a; Kaur et al., 2023; Yang et al., 2024a; Yang et al., 2024b). Since Biot (1956) established the wave propagation theory for single-phase thermoelastic solid media, studies on the characteristics of thermoelastic wave propagation have gradually become systematic. Based on this, Pecker (1973) developed wave equations for saturated porous thermoelastic media, revealing the existence of thermal waves under non-isothermal conditions, similar to those in thermoelastic solids. This phenomenon was experimentally confirmed in studies by Berryman (1980), Plona (1980), and Johnson et al. (1994). Building on this work, Liu et al. (2009) and Liu et al. (2016) developed a fully coupled nonlinear thermo-hydro-mechanical model for saturated porous media, incorporating the influence of temperature on fluid flow and other factors. Interfaces between media affect wave propagation, causing phenomena such as transmission and reflection. Zheng et al. (2013; 2014) and Liu et al. (2020b) investigated the reflection characteristics of SV-waves at interfaces and analyzed the influence of thermophysical parameters on wave velocity. However, research on the thermo-hydro-mechanical coupled wave theory for unsaturated soils—commonly encountered in engineering—remains relatively limited, particularly regarding the seismic response characteristics of complex sites under thermo-hydro-mechanical coupling. Building on achievements in isothermal models, Liu et al. (2021) and Zhou et al. (2020) established thermoelastic wave equations for unsaturated soils and analyzed the influence of thermodynamic parameters on wave velocity and amplitude reflection ratio. Yang et al. (2023; 2024c) further developed models for SV-wave incidence in single-phase–unsaturated soil and homogeneous layered elastic foundations, studying the influence of physical parameters on surface displacement amplification factors under different angles of incidence. These works have advanced research on the seismic response of complex sites under thermoelastic wave incidence.

Based on thermo-elastic wave theory, this study establishes a bedrock-saturated soil-unsaturated soil site model to investigate the characteristics of seismic wave propagation under non-isothermal conditions. Using the Helmholtz decomposition theorem and incorporating appropriate boundary conditions, an analytical solution for the seismic response of the site under SV-wave incidence at arbitrary angles is derived. Numerical simulations are conducted to systematically examine the influence of key parameters such as groundwater level, degree of saturation, and thermal conductivity coefficient on surface displacements. The results provide a theoretical basis for seismic response analysis of geo-structural sites under non-isothermal conditions.

2 The fluctuation equations for the site

In order to study the seismic response of bedrock-saturated soil-unsaturated site under thermal effect, this section will establish the wave equations of three media in turn. Although the governing equations of each medium are different, the wavenumber solving process follows a unified mathematical path. As a key parameter to characterize the wave propagation characteristics, the wave number directly affects the wave velocity and attenuation behavior, and plays an important role in accurately calculating the seismic ground motion response of the site.

2.1 *Equations of motion for monophase thermoelastic media*

The rock layer is considered a single-phase thermoelastic medium, whose wave equation under the general theory of thermo-elasticity is given by Liu (2024a):

$$\mu_{\mathrm{e}}\nabla^2 u^{\mathrm{s}} + (\lambda_{\mathrm{e}} + \mu_{\mathrm{e}})\nabla\left(\nabla \cdot u^{\mathrm{s}}\right) - 3K_{b\mathrm{e}}\beta_{T\mathrm{e}}\nabla\phi_{\mathrm{e}} = \rho_{\mathrm{e}}\ddot{u}^{\mathrm{s}} \tag{1a}$$

$$3K_{b\mathrm{e}}\beta_{T\mathrm{e}}T_{\mathrm{e}0}\nabla\cdot\left(\dot{u}^{\mathrm{s}} + \tau_{q\mathrm{e}}\ddot{u}^{\mathrm{s}}\right) + \rho^{\mathrm{e}}c_{s\mathrm{e}}\left(\dot{\phi}_{\mathrm{e}} + \tau_{q\mathrm{e}}\ddot{\phi}_{\mathrm{e}}\right) = K_{\mathrm{e}}\nabla^2\left(\phi_{\mathrm{e}} + \tau_{\theta\mathrm{e}}\dot{\phi}_{\mathrm{e}}\right) \tag{1b}$$

In the formula: the subscript e represents the single-phase elastic medium; $K_{b\mathrm{e}} = (\lambda_{\mathrm{e}} + 2\mu_{\mathrm{e}} / 3)$ represents the bulk modulus; λ_{e} and μ_{e} are the lame constants of the elastic medium, respectively. The density of the elastic medium is expressed by ρ_{e} ; the thermophysical parameters of solid phase heat, thermal conductivity, coefficient of thermal expansion, phase delay time of heat flow and phase delay time of temperature gradient are expressed by $c_{s\mathrm{e}}$, K_{e}, $\beta_{T\mathrm{e}}$, $\tau_{q\mathrm{e}}$, $\tau_{\theta\mathrm{e}}$ respectively. T_{e} and $T_{\mathrm{e}0}$ represent the temperature of the Kelvin medium and the initial temperature, respectively. u^{s} represents the displacement vector of the solid medium.

Through Helmholtz vector decomposition, the displacement vector field is decomposed into scalar potential and vector potential, and the coupled vector equation is transformed into a scalar equation that is easier to solve. Its decomposition form is:

$$u^{\mathrm{s}} = \nabla\psi_{\mathrm{s}} + \nabla\times H_{\mathrm{s}} \tag{2}$$

To construct the general solution of the wave equation, the potential function of the wave is assumed to be:

$$\psi_{\mathrm{s}} = A_{\mathrm{s}}\exp[\mathrm{i}(k_{\mathrm{pe}}x - \omega t)] \tag{3a}$$

$$H_{\mathrm{s}} = B_{\mathrm{s}}\exp[\mathrm{i}(k_{s\mathrm{e}}x - \omega t)] \tag{3b}$$

$$\phi = A^{\mathrm{T}}\exp[\mathrm{i}(k_{\mathrm{pe}}x - \omega t)] \tag{3c}$$

where A_{s}, A^{T}, B_{s} represent the amplitude coefficients of P-wave (including T-wave) and S-wave, respectively; k_{pe} and $k_{s\mathrm{e}}$ represent the wave numbers of P-wave and S-wave; ω denotes the frequency.

In order to solve the wave number of each wave, the formula (2) is substituted into the formula (1) and combined with the formula (3), and the dispersion characteristic equation of the body wave in the thermoelastic solid medium is derived as follows:

$$\begin{vmatrix} k_{\mathrm{e}11} & k_{\mathrm{e}12} \\ k_{\mathrm{e}21} & k_{\mathrm{e}22} \end{vmatrix} = 0 \tag{4}$$

$$\left| \rho_{\mathrm{e}}\omega^2 - \mu_{\mathrm{e}}k_{\mathrm{se}}^2 \right| = 0 \tag{5}$$

Eq. (4) represents the characteristic equation of a compression wave, which includes the T wave, and Eq. (5) represents the characteristic equation of a shear wave, which is also called an S wave. The expressions $k_{\mathrm{e}11}$, $k_{\mathrm{e}12}$, $k_{\mathrm{e}21}$, $k_{\mathrm{e}22}$ are described in Appendix A.

2.2 *Equations of motion for saturated porous thermoelastic media*

Based on the generalized thermo-elastic theory, the wave equation for a saturated porous thermo-elastic medium was proposed by Liu (2020a).

$$\mu_{\mathrm{v}}\nabla^2 u^{\mathrm{s}} + (b_{\mathrm{v}11} + \mu_{\mathrm{v}})\nabla\left(\nabla \cdot u^{\mathrm{s}}\right) + b_{\mathrm{v}12}\nabla\left(\nabla \cdot u^{\mathrm{l}}\right) + b_{\mathrm{v}13}\nabla\phi_{\mathrm{v}} = \rho_{\mathrm{v}t}\ddot{u}^{\mathrm{s}} + \rho_{\mathrm{v}l}\ddot{u}^{\mathrm{l}} \tag{6a}$$

$$b_{\mathrm{v}21}\nabla\left(\nabla \cdot u^{\mathrm{s}}\right) + b_{\mathrm{v}22}\nabla\left(\nabla \cdot u^{\mathrm{l}}\right) + b_{\mathrm{v}23}\nabla\phi_{\mathrm{v}} = \rho_{\mathrm{v}l}\ddot{u}^{\mathrm{s}} + \vartheta_{\mathrm{v}l}\ddot{u}^{\mathrm{l}} + \nu_{\mathrm{v}l}\dot{u}^{\mathrm{l}} \tag{6b}$$

$$b_{\mathrm{v}31}\nabla \cdot \left(\dot{u}^{\mathrm{s}} + \tau_{q\mathrm{v}}\ddot{u}^{\mathrm{s}}\right) + b_{\mathrm{v}32}\nabla \cdot \left(\dot{u}^{\mathrm{l}} + \tau_{q\mathrm{v}}\ddot{u}^{\mathrm{l}}\right) + b_{\mathrm{v}33}(\dot{\phi}_{\mathrm{v}} + \tau_{q\mathrm{v}}\ddot{\phi}_{\mathrm{v}}) = K_{\mathrm{v}}\nabla^2(\phi_{\mathrm{v}} + \tau_{\theta\mathrm{v}}\dot{\phi}_{\mathrm{v}}) \tag{6c}$$

where

$$\rho_{\mathrm{v}t} = \rho_{\mathrm{v}s} + \rho_{\mathrm{v}l}, b_{\mathrm{v}11} = \lambda_{\mathrm{v}} + \alpha_{\mathrm{v}}(a_{\mathrm{v}11} + a_{\mathrm{v}12}), b_{\mathrm{v}12} = \alpha_{\mathrm{v}}a_{\mathrm{v}12} / n_{\mathrm{v}s}, b_{\mathrm{v}13} = \alpha_{\mathrm{v}}a_{\mathrm{v}13} - \lambda_{\mathrm{v}}^{'}, b_{\mathrm{v}21} = a_{\mathrm{v}11} + a_{\mathrm{v}12}, b_{\mathrm{v}22} = a_{\mathrm{v}12} / n_{\mathrm{v}s},$$

$$b_{\mathrm{v}23} = a_{\mathrm{v}13}, b_{\mathrm{v}31} = (\lambda_{\mathrm{v}}^{'} + \beta_{T\mathrm{v}}b_{\mathrm{v}21})T_{\mathrm{v}0}, b_{\mathrm{v}32} = \beta_{T\mathrm{v}}T_{\mathrm{v}0}b_{\mathrm{v}22}, b_{\mathrm{v}33} = \tilde{m}_{\mathrm{v}s} + \beta_{T\mathrm{v}}T_{\mathrm{v}0}b_{\mathrm{v}23}$$

The saturated porous medium is represented by v; λ_{v} and μ_{v} are the Lame constants of the saturated porous media, respectively. $\rho_{\mathrm{v}t}$ denotes the density of the saturated porous media; $n_{\mathrm{v}s}$ represents the porosity of the saturated porous media; the thermophysical parameters $\tau_{q\mathrm{v}}$, $\tau_{\theta\mathrm{v}}$, K_{v} and $\beta_{T\mathrm{v}}$ represent the heat flow phase delay time, the temperature flux phase delay time, the thermal conductivity and the thermal expansion coefficient of the saturated porous media, respectively. T_{v} and $T_{\mathrm{v}0}$ represent the Kelvin medium temperature and the initial temperature. u^{s} represents the displacement vector of the solid medium; u^{l} denotes the relative displacement of the liquid phase with respect to the solid skeleton. Further expressions are given in reference (Liu 2020a).

The Helmholtz potential function decomposition form of the displacement vector of the solid phase and the liquid phase medium is introduced. That is, through the Helmholtz vector decomposition, the displacement vector field is decomposed into scalar potential and vector potential, and the coupled vector equation is transformed into a scalar equation that is easier to solve. Its decomposition form is:

$$u^{\mathrm{s}} = \nabla\psi_{\mathrm{s}} + \nabla \times H_{\mathrm{s}} \tag{7a}$$

$$u^{\mathrm{l}} = \nabla\psi_{\mathrm{l}} + \nabla \times H_{\mathrm{l}} \tag{7b}$$

In order to construct the general solution of the thermoelastic wave equation of saturated porous media, the potential function of the wave is assumed as:

$$\psi_{\alpha} = A_{\alpha} \exp[\mathrm{i}(k_{\mathrm{pv}}x - \omega t)] \tag{8a}$$

$$H_{\alpha} = B_{\alpha} \exp[\mathrm{i}(k_{\mathrm{sv}}x - \omega t)] \tag{8b}$$

$$\phi = A^{\mathrm{T}} \exp[\mathrm{i}(k_{\mathrm{pv}}x - \omega t)] \tag{8c}$$

where $A_{\alpha}(\alpha = \mathrm{s,l})$, A^{T}, B_{α} represent the amplitude coefficients of P-wave (including T-wave) and S-wave, respectively; k_{pv} and k_{sv} denote the wave numbers of compressional and shear waves.

Combined with the assumption of the potential function, it is substituted into the wave equation to obtain the dispersion characteristic equation of the thermoelastic wave in the saturated porous medium, which is used to obtain the wave number of each wave.

$$\begin{vmatrix} b_{\mathrm{v}t11} & b_{\mathrm{v}t12} & b_{\mathrm{v}t13} \\ b_{\mathrm{v}t21} & b_{\mathrm{v}t22} & b_{\mathrm{v}t23} \\ b_{\mathrm{v}t31} & b_{\mathrm{v}t32} & b_{\mathrm{v}t33} \end{vmatrix} = 0 \tag{9}$$

$$\begin{vmatrix} c_{\mathrm{v}t11} & c_{\mathrm{v}t12} \\ c_{\mathrm{v}t21} & c_{\mathrm{v}t22} \end{vmatrix} = 0 \tag{10}$$

Equation (9) is the dispersion equation of the P-wave (including the T-wave), and equation (10) is the dispersion equation of the S-wave. The expressions $b_{\mathrm{v}t11}$, $b_{\mathrm{v}t12}$, $b_{\mathrm{v}t13}$, $b_{\mathrm{v}t21}$, $b_{\mathrm{v}t22}$, $b_{\mathrm{v}t23}$, $b_{\mathrm{v}t31}$, $b_{\mathrm{v}t32}$, $b_{\mathrm{v}t33}$, $c_{\mathrm{v}t11}$, $c_{\mathrm{v}t12}$, $c_{\mathrm{v}t21}$, $c_{\mathrm{v}t22}$ are described in Appendix A.

By solving the characteristic equation, six different complex wave numbers can be derived from equation (9), and two different complex wave numbers can be derived from equation (10). Then the wave velocity of compressive wave and shear wave can be obtained.

2.2 *Equations of motion for unsaturated porous thermoelastic media*

The relative displacements u^{l} and u^{g} of the liquid and gas phases with respect to the solid skeleton are introduced. According to the thermoelastic theory of porous media, the wave equation of unsaturated porous thermoelastic media is obtained as (Liu 2020a):

$$\mu_{\mathrm{u}}\nabla^2 u^{\mathrm{s}} + (\overline{\lambda}_{\mathrm{u}} + \mu_{\mathrm{u}})\nabla(\nabla \cdot u^{\mathrm{s}}) + D_1\nabla(\nabla \cdot u^{\mathrm{l}}) + D_2\nabla(\nabla \cdot u^{\mathrm{g}}) + D_3\nabla\phi_{\mathrm{u}} = \rho_{\mathrm{u}}\ddot{u}^{\mathrm{s}} + \rho_{\mathrm{ul}}\ddot{u}^{\mathrm{l}} + \rho_{\mathrm{ug}}\ddot{u}^{\mathrm{g}} \tag{11a}$$

$$B_1\nabla(\nabla \cdot u^{\mathrm{s}}) + B_2\nabla(\nabla \cdot u^{\mathrm{l}}) + B_3\nabla(\nabla \cdot u^{\mathrm{g}}) + B_4\nabla\phi_{\mathrm{u}} = \rho_{\mathrm{ul}}\ddot{u}^{\mathrm{s}} + \vartheta_{\mathrm{ul}}\ddot{u}^{\mathrm{l}} + \nu_{\mathrm{ul}}\dot{u}^{\mathrm{l}} \tag{11b}$$

$$B_5\nabla(\nabla \cdot u^{\mathrm{s}}) + B_6\nabla(\nabla \cdot u^{\mathrm{l}}) + B_7\nabla(\nabla \cdot u^{\mathrm{g}}) + B_8\nabla\phi_{\mathrm{u}} = \rho_{\mathrm{ug}}\ddot{u}^{\mathrm{s}} + \vartheta_{\mathrm{ug}}\ddot{u}^{\mathrm{g}} + \nu_{\mathrm{ug}}\dot{u}^{\mathrm{g}} \tag{11c}$$

$$C_1\nabla \cdot (\dot{u}^{\mathrm{s}} + \tau_{q\mathrm{u}}\ddot{u}^{\mathrm{s}}) + C_2\nabla \cdot (\dot{u}^{\mathrm{l}} + \tau_{q\mathrm{u}}\ddot{u}^{\mathrm{l}}) + C_3\nabla \cdot (\dot{u}^{\mathrm{g}} + \tau_{q\mathrm{u}}\ddot{u}^{\mathrm{g}}) + C_4(\dot{\phi}_{\mathrm{u}} + \tau_{q\mathrm{u}}\ddot{\phi}_{\mathrm{u}}) = K_{\mathrm{u}}\nabla^2(\phi_{\mathrm{u}} + \tau_{\theta\mathrm{u}}\dot{\phi}_{\mathrm{u}}) \tag{11d}$$

The expressions D_1, D_2, D_3, C_1, C_2, C_3, C_4 are described in Appendix A.

Unsaturated porous media are represented by u, where λ_{u} and μ_{u} are the Lame constants of unsaturated porous media. γ is the effective stress parameter, which represents the proportion of the contribution of matrix suction to the effective stress. ρ_{u} is the total density of unsaturated porous media, which is the synthesis of the apparent densities of the solid, liquid and gas phases. n_{us} represents the porosity of unsaturated porous media; The thermophysical parameters K_{u}, $\tau_{q\mathrm{u}}$, $\tau_{\theta\mathrm{u}}$ and $\beta_{T\mathrm{u}}$ represent the thermal conductivity, the heat flow phase delay time, the temperature gradient phase delay time and the thermal expansion coefficient of the unsaturated porous medium, respectively. T_{u0} denotes the initial temperature; u^{s}, u^{l} and u^{g} represent solid, liquid and gas phase displacement vectors respectively. In addition, other expressions are given in the reference (Liu 2020a).

In order to decouple the vector wave equation of solid-liquid-gas three-phase coupling, based on the Helmholtz vector decomposition principle, the displacement field of each phase is decomposed into scalar potential and vector potential, so that the original control equation is transformed into a scalar form which is easy to solve. Its decomposition form can be expressed as:

$$u^{\mathrm{s}} = \nabla\psi_{\mathrm{s}} + \nabla \times H_{\mathrm{s}} \tag{12a}$$

$$u^{\mathrm{l}} = \nabla\psi_{\mathrm{l}} + \nabla \times H_{\mathrm{l}} \tag{12b}$$

$$u^{\mathrm{g}} = \nabla\psi_{\mathrm{g}} + \nabla \times H_{\mathrm{g}} \tag{12c}$$

In order to construct the general solution of the thermoelastic wave equation of unsaturated porous media, the potential function of the wave is assumed as:

$$\psi_{\beta} = A_{\beta}\exp[(\mathrm{i}k_{\mathrm{pu}}x - \omega t)] \tag{13a}$$

$$H_{\beta} = B_{\beta}\exp[\mathrm{i}(k_{\mathrm{su}}x - \omega t)] \tag{13b}$$

$$\phi = A^{\mathrm{T}}\exp[\mathrm{i}(k_{\mathrm{pu}}x - \omega t)] \tag{13c}$$

where $A_{\beta}(\beta = \mathrm{s},\mathrm{l},\mathrm{g})$, A^{T}, B_{β} represent the amplitude coefficients of P-wave (including T-wave) and S-wave, respectively; k_{pu} and k_{su} denote the wave numbers of compressional and shear waves.

In order to determine the wave number of each wave in unsaturated porous media, the potential function is introduced into the wave equation, and then the corresponding thermoelastic dispersion characteristic equation is derived.

$$\begin{vmatrix} bb_{\mathrm{u11}} & bb_{\mathrm{u12}} & bb_{\mathrm{u13}} & bb_{\mathrm{u14}} \\ bb_{\mathrm{u21}} & bb_{\mathrm{u22}} & bb_{\mathrm{u23}} & bb_{\mathrm{u24}} \\ bb_{\mathrm{u31}} & bb_{\mathrm{u32}} & bb_{\mathrm{u33}} & bb_{\mathrm{u34}} \\ bb_{\mathrm{u41}} & bb_{\mathrm{u42}} & bb_{\mathrm{u43}} & bb_{\mathrm{u44}} \end{vmatrix} = 0 \tag{14}$$

$$\begin{vmatrix} c_{\mathrm{u}11} & c_{\mathrm{u}12} & c_{\mathrm{u}13} \\ c_{\mathrm{u}21} & c_{\mathrm{u}22} & c_{\mathrm{u}23} \\ c_{\mathrm{u}31} & c_{\mathrm{u}32} & c_{\mathrm{u}33} \end{vmatrix} = 0 \tag{15}$$

Eq. (14) is the P-wave dispersion equation (including T-wave), and Eq. (15) is the S-wave dispersion equation, where the elements are:

$$bb_{\mathrm{u}11} = \rho_{\mathrm{u}}\omega^2 - (\overline{\lambda}_{\mathrm{u}} + 2\mu_{\mathrm{u}})k_{\mathrm{pu}}^2, bb_{\mathrm{u}12} = \rho_{\mathrm{ul}}\omega^2 - D_1 k_{\mathrm{pu}}^2, bb_{\mathrm{u}13} = \rho_{\mathrm{ug}}\omega^2 - D_2 k_{\mathrm{pu}}^2, b_{\mathrm{u}14} = D_3, bb_{\mathrm{u}21} = \rho_{\mathrm{ul}}\omega^2 - B_1 k_{\mathrm{pu}}^2$$
$$bb_{\mathrm{u}22} = \vartheta_{\mathrm{u}l}\omega^2 + \nu_{\mathrm{u}l}\mathrm{i}\omega - B_2 k_{\mathrm{pu}}^2, bb_{\mathrm{u}23} = -B_3 k_{\mathrm{pu}}^2, bb_{\mathrm{u}24} = B_4, bb_{\mathrm{u}31} = \rho_{\mathrm{ug}}\omega^2 - B_5 k_{\mathrm{pu}}^2, b_{\mathrm{u}33} = \vartheta_{\mathrm{u}g}\omega^2 + \nu_{\mathrm{u}g}\mathrm{i}\omega - B_7 k_{\mathrm{pu}}^2$$
$$bb_{\mathrm{u}32} = -B_6 k_{\mathrm{pu}}^2, bb_{\mathrm{u}34} = B_8, bb_{\mathrm{u}41} = C_1(\mathrm{i}\omega + \tau_{q\mathrm{u}}\omega^2)k_{\mathrm{pu}}^2, bb_{\mathrm{u}42} = C_2(\mathrm{i}\omega + \tau_{q\mathrm{u}}\omega^2)k_{\mathrm{pu}}^2, bb_{\mathrm{u}43} = C_3(\mathrm{i}\omega + \tau_{q\mathrm{u}}\omega^2)k_{\mathrm{pu}}^2$$
$$bb_{\mathrm{u}44} = K_{\mathrm{u}}(1 - \tau_{\theta\mathrm{u}}\mathrm{i}\omega)k_{\mathrm{pu}}^2 - C_4(\mathrm{i}\omega + \tau_{q\mathrm{u}}\omega^2)$$

Eight different complex wave numbers can be solved from formula (14), and two different complex wave numbers can be solved from formula (15). Other expressions are also given in reference (Liu 2020a).

3 Analysis of the wave field

In order to solve the displacement amplification factor that characterizes the dynamic response of the site, this section will perform wave field analysis based on the aforementioned model. Firstly, the potential function of wave in each medium is established. Then, the Snell theorem is used to coordinate the wave vector, and the complete stress-displacement boundary condition is used to construct the equation set for solving the amplitude coefficient. The solution of the equation set determines the surface displacement amplification factor of the site.

Under the assumption that the plane S wave with a frequency of ω is incident at any angle θ_{is} from the rock layer to the interface of the rock-saturated porous thermoelastic medium, As shown in Figure1, three kinds of reflected waves (reflected P wave, reflected S wave, reflected T wave) are generated in the rock layer, and four kinds of transmitted waves and four kinds of reflected waves are generated in the saturated soil layer. As the seismic wave propagates further in the soil layer, five kinds of transmitted waves and five kinds of reflected waves (reflected P1 wave, reflected P2 wave, reflected P3 wave, reflected T wave, reflected S wave) will be generated in the unsaturated porous thermoelastic medium.

3.1 *Solution in a homogeneous layer*

The wave field functions of single-phase medium, saturated porous medium and unsaturated porous medium are expressed as follows, which lays a foundation for the subsequent coupling solution of amplitude coefficient.

Body wave potential function in monophase thermoelastic medium:

$$\psi_{\mathrm{e}} = \sum_{n=1}^{2} A_{\mathrm{serp}n} \exp[\mathrm{i}k_{\mathrm{erp}n}(l_{\mathrm{erp}n}x + n_{\mathrm{erp}n}z - c_{\mathrm{erp}n}t)] \tag{16}$$

$$\phi_{\mathrm{e}} = \sum_{n=1}^{2} A_{\mathrm{serp}n} \exp[\mathrm{i}k_{\mathrm{erp}n}(l_{\mathrm{erp}n}x + n_{\mathrm{erp}n}z - c_{\mathrm{erp}n}t)] \tag{17}$$

$$H_{\mathrm{e}} = B_{\mathrm{is}} \exp[\mathrm{i}k_{\mathrm{is}}(l_{\mathrm{is}}x - n_{\mathrm{is}}z - c_{\mathrm{is}}t)] + B_{\mathrm{ers}} \exp[\mathrm{i}k_{\mathrm{ers}}(l_{\mathrm{ers}}x + n_{\mathrm{ers}}z - c_{\mathrm{ers}}t)] \tag{18}$$

Body wave potential in saturated porous thermoelastic medium:

$$\psi_{\mathrm{v}}^{\alpha}=\sum_{n=1}^{3}A_{\alpha\mathrm{vtp}n}\exp[\mathrm{i}k_{\mathrm{vtp}n}(l_{\mathrm{vtp}n}x-n_{\mathrm{vtp}n}z-c_{\mathrm{vtp}n}t)]+\sum_{n=1}^{3}A_{\alpha\mathrm{vrp}n}\exp[\mathrm{i}k_{\mathrm{vrp}n}(l_{\mathrm{vrp}n}x-n_{\mathrm{vrp}n}z-c_{\mathrm{vrp}n}t)] \tag{19}$$

$$\phi_{\mathrm{v}}=\sum_{n=1}^{3}A_{\mathrm{svtp}n}\delta_{\mathrm{vTp}n}\exp[\mathrm{i}k_{\mathrm{vtp}n}(l_{\mathrm{vtp}n}x-n_{\mathrm{vtp}n}z-c_{\mathrm{vtp}n}t)]+\sum_{n=1}^{3}A_{\mathrm{svrp}n}\delta_{\mathrm{vTp}n}\exp[\mathrm{i}k_{\mathrm{vrp}n}(l_{\mathrm{vrp}n}x+n_{\mathrm{vrp}n}z-c_{\mathrm{vrp}n}t)] \tag{20}$$

$$H_{\mathrm{v}}^{\alpha}=B_{\alpha\mathrm{vts}}\exp[\mathrm{i}k_{\mathrm{vts}}(l_{\mathrm{vts}}x-n_{\mathrm{vts}}z-c_{\mathrm{vts}}t)]+B_{\alpha\mathrm{vrs}}\exp[\mathrm{i}k_{\mathrm{vrs}}(l_{\mathrm{vrs}}x+n_{\mathrm{vrs}}z-c_{\mathrm{vrs}}t)] \tag{21}$$

Body wave potential in unsaturated porous thermoelastic media:

$$\psi_{\mathrm{u}}^{\beta}=\sum_{n=1}^{4}A_{\beta\mathrm{utp}n}\exp[\mathrm{i}k_{\mathrm{utp}n}(l_{\mathrm{utp}n}x-n_{\mathrm{utp}n}z-c_{\mathrm{utp}n}t)]+\sum_{n=1}^{4}A_{\beta\mathrm{urp}n}\exp[\mathrm{i}k_{\mathrm{urp}n}(l_{\mathrm{urp}n}x+n_{\mathrm{urp}n}z-c_{\mathrm{urp}n}t)] \tag{22}$$

$$\phi_{\mathrm{u}}=\sum_{n=1}^{4}A_{\mathrm{sutp}n}\delta_{\mathrm{uTp}n}\exp[\mathrm{i}k_{\mathrm{utp}n}(l_{\mathrm{utp}n}x-n_{\mathrm{utp}n}z-c_{\mathrm{utp}n}t)]+\sum_{n=1}^{4}A_{\mathrm{surp}n}\delta_{\mathrm{uTp}n}\exp[\mathrm{i}k_{\mathrm{urp}n}(l_{\mathrm{urp}n}x+n_{\mathrm{urp}n}z-c_{\mathrm{urp}n}t)] \tag{23}$$

$$H_{\mathrm{u}}^{\beta}=B_{\beta\mathrm{uts}}\exp[\mathrm{i}k_{\mathrm{uts}}(l_{\mathrm{uts}}x-n_{\mathrm{uts}}z-c_{\mathrm{uts}}t)]+B_{\beta\mathrm{urs}}\exp[\mathrm{i}k_{\mathrm{urs}}(l_{\mathrm{urs}}x+n_{\mathrm{urs}}z-c_{\mathrm{urs}}t)] \tag{24}$$

where ψ, ϕ and H represent the potential functions of P-wave, T-wave and S-wave respectively; the subscripts e, v and u represent single-phase thermoelastic media, saturated porous thermoelastic media and unsaturated porous thermoelastic media respectively. The subscripts i, r and t denote incident wave, reflected wave and transmitted wave, respectively. A and B represent the amplitude coefficients of P-wave (including T-wave) and S-wave, respectively. The solid-liquid two-phase in saturated porous media is represented by $\alpha(\alpha=\mathrm{s},\mathrm{l})$. A three-dimensional representation of the solid-liquid-gas phase behavior in unsaturated porous media is given by the symbol $\beta(\beta=\mathrm{s},\mathrm{l},\mathrm{g})$. k_{is} and c_{is} represent wave numbers and wave velocities of incident S-waves, respectively. $k_{\mathrm{erp}n}$, k_{ers}, $c_{\mathrm{erp}n}$, c_{ers} represent wave numbers and corresponding wave velocities of reflected compression waves and reflected shear waves in single-phase media, respectively. $k_{\mathrm{vtp}n}$, k_{vts}, $c_{\mathrm{vtp}n}$, c_{vts}, $k_{\mathrm{vrp}n}$, k_{vrs}, $c_{\mathrm{vrp}n}$, c_{vrs} represent the wave number and wave velocity of transmission compression wave and transmission shear wave in saturated porous media, and the wave number and wave velocity of reflection compression wave and reflection shear wave, respectively. $k_{\mathrm{utp}n}$, k_{uts}, $c_{\mathrm{utp}n}$, c_{uts}, $k_{\mathrm{urp}n}$, k_{urs}, $c_{\mathrm{urp}n}$, c_{urs} represent the wave numbers and wave velocities of the transmissive compression wave and transmissive shear wave, and the wave numbers and wave velocities of the reflective compression wave and reflective shear wave in unsaturated porous materials, respectively. *l* and *n* are the directional vectors in the *x* and *z* direction, respectively.

According to Snell 's theorem, at the interface of adjacent medium layers (single-phase and saturated soil layer, saturated soil and unsaturated soil layer), the horizontal wave number of each body wave must be equal to meet the condition of phase matching in the propagation process, that is:

$$\begin{aligned}&\boldsymbol{l}_{\mathrm{is}}k_{\mathrm{is}}=\boldsymbol{l}_{\mathrm{erp1}}k_{\mathrm{erp1}}=\boldsymbol{l}_{\mathrm{erp2}}k_{\mathrm{erp2}}=\boldsymbol{l}_{\mathrm{ers}}k_{\mathrm{ers}}=\boldsymbol{l}_{\mathrm{vrp1}}k_{\mathrm{vrp1}}=\boldsymbol{l}_{\mathrm{vrp2}}k_{\mathrm{vrp2}}=\boldsymbol{l}_{\mathrm{vrp3}}k_{\mathrm{vrp3}}=\boldsymbol{l}_{\mathrm{vtp1}}k_{\mathrm{vtp1}}=\\&\boldsymbol{l}_{\mathrm{vtp2}}k_{\mathrm{vtp2}}=\boldsymbol{l}_{\mathrm{vtp3}}k_{\mathrm{vtp3}}=\boldsymbol{l}_{\mathrm{vts}}k_{\mathrm{vts}}=\boldsymbol{l}_{\mathrm{vrs}}k_{\mathrm{vrs}}=\boldsymbol{l}_{\mathrm{uts}}k_{\mathrm{uts}}=\boldsymbol{l}_{\mathrm{urs}}k_{\mathrm{urs}}=\boldsymbol{l}_{\mathrm{urp1}}k_{\mathrm{urp1}}=\boldsymbol{l}_{\mathrm{urp2}}k_{\mathrm{urp2}}=\\&\boldsymbol{l}_{\mathrm{urp3}}k_{\mathrm{urp3}}=\boldsymbol{l}_{\mathrm{urp4}}k_{\mathrm{urp4}}=\boldsymbol{l}_{\mathrm{utp1}}k_{\mathrm{utp1}}=\boldsymbol{l}_{\mathrm{utp2}}k_{\mathrm{utp2}}=\boldsymbol{l}_{\mathrm{utp3}}k_{\mathrm{utp3}}=\boldsymbol{l}_{\mathrm{utp4}}k_{\mathrm{utp4}}\end{aligned} \tag{25}$$

In order to simplify the solution, the proportional relationship of potential function amplitude is introduced to greatly reduce the number of unknowns and reduce the computational complexity, which is the key prerequisite for constructing solvable equations.

From formula (4) and formula (5) the ratio of the amplitude of the potential function of the P-wave and the T-wave in the single-phase thermoelastic medium is derived.

$$\delta_{\mathrm{eTp}n}=\frac{A_{\mathrm{p}}^{\mathrm{T}}}{A_{\mathrm{p}}^{\mathrm{S}}}=-\frac{k_{\mathrm{e11}}}{k_{\mathrm{e12}}} \tag{26}$$

From formula (4), two meaningful solutions can be obtained, which are not the general solution of the dispersion characteristic equation, but the specific solution applicable to the site model, corresponding to *n* = 1,2 respectively. T-wave and S-wave potential functions in a saturated porous thermoelastic medium can be derived from Eq. (9) and Eq. (10) as follows:

$$\delta_{\mathrm{vlp}n}=\frac{A_{\mathrm{l}n}}{A_{\mathrm{s}n}}=\frac{b_{\mathrm{v}t11n}b_{\mathrm{v}t23n}-b_{\mathrm{v}t21n}b_{\mathrm{v}t13n}}{b_{\mathrm{v}t22n}b_{\mathrm{v}t13n}-b_{\mathrm{v}t12n}b_{\mathrm{v}t23n}} \tag{27a}$$

$$\delta_{\mathrm{vTp}n}=\frac{A_{\mathrm{T}n}}{A_{\mathrm{s}n}}=\frac{b_{\mathrm{v}t32n}b_{\mathrm{v}t21n}-b_{\mathrm{v}t22n}b_{\mathrm{v}t31n}}{b_{\mathrm{v}t22n}b_{\mathrm{v}t33n}-b_{\mathrm{v}t23n}b_{\mathrm{v}t32n}} \tag{27b}$$

$$\delta_{\mathrm{vls}}=\frac{B_{\mathrm{l}}}{B_{\mathrm{s}}}=-\frac{c_{\mathrm{v}t21}}{c_{\mathrm{v}t22}} \tag{27c}$$

Three effective solutions are obtained from Equation (9). This solution is not the general solution of the dispersion characteristic equation, but the special solution under the site model, then *n* = 1, 2, 3. The ratio of the amplitude of the potential function of the P-wave and the T-wave in the unsaturated porous thermoelastic medium is derived from the equation (14) and the equation (15):

$$\delta_{\mathrm{ulp}n}=\frac{A_{\mathrm{l}n}}{A_{\mathrm{s}n}}=\frac{d_{11n}d_{15n}-d_{12n}d_{16n}}{d_{13n}d_{16n}-d_{14n}d_{15n}} \tag{28a}$$

$$\delta_{\mathrm{ugp}n}=\frac{A_{\mathrm{g}n}}{A_{\mathrm{s}n}}=\frac{d_{21n}d_{25n}-d_{22n}d_{26n}}{d_{23n}d_{26n}-d_{24n}d_{25n}} \tag{28b}$$

$$\delta_{\mathrm{uTp}n}=\frac{A_{\mathrm{T}n}}{A_{\mathrm{s}n}}=\frac{d_{31n}d_{35n}-d_{32n}d_{36n}}{d_{33n}d_{36n}-d_{34n}d_{35n}} \tag{28c}$$

$$\delta_{\mathrm{uls}}=\frac{B_{\mathrm{l}}}{B_{\mathrm{s}}}=-\frac{c_{\mathrm{u}12}}{c_{\mathrm{u}22}} \tag{28d}$$

$$\delta_{\mathrm{ugs}}=\frac{B_{\mathrm{g}}}{B_{\mathrm{s}}}=\frac{c_{\mathrm{u}21}c_{\mathrm{u}12}-c_{\mathrm{u}11}c_{\mathrm{u}22}}{c_{\mathrm{u}13}c_{\mathrm{u}22}} \tag{28e}$$

There are four meaningful solutions to the dispersion characteristic equation (14), which represent three kinds of body waves (three kinds of compression waves and thermal waves) in the model. Therefore, *n* = 1, 2, 3, 4. The expressions d_{11n}, d_{12n}, d_{13n}, d_{14n}, d_{15n}, d_{16n}, d_{21n}, d_{22n}, d_{23n}, d_{24n}, d_{25n}, d_{26n}, d_{31n}, d_{32n}, d_{33n}, d_{34n}, d_{35n}, d_{36n} are described in Appendix A.

3.2 *Boundary condition*

The incident S wave amplitude is set to 1, and the site contains 21 unknown wave amplitude coefficients (3 in bedrock layer, 7 in saturated soil layer and 11 in unsaturated soil layer). In order to solve all the unknowns, 21 independent equations need to be established. Through the stress-displacement continuous boundary conditions at each interface, the linear equations are established. Among them, the interface between the bedrock layer and the saturated soil layer is treated as impermeable, the interface between the saturated soil layer and the unsaturated soil layer is permeable, and the surface is a free permeable and adiabatic boundary. Through the boundary conditions of stress displacement continuity and temperature continuity, the amplitude coefficient of each wave can be determined, and then the seismic ground motion response of the site can be analyzed.

The boundary constraints at the junction between the single-phase thermoelastic and saturation thermoelastic media at z=H1 are as follows:

$$u_{\mathrm{e}xz}^{\mathrm{s}}=u_{\mathrm{v}xz}^{\mathrm{s}},u_{\mathrm{e}zz}^{\mathrm{s}}=u_{\mathrm{v}zz}^{\mathrm{s}},u_{\mathrm{v}zz}^{\mathrm{s}}=u_{\mathrm{v}zz}^{\mathrm{l}},\sigma_{\mathrm{e}xz}^{\mathrm{s}}=\sigma_{\mathrm{v}xz}^{\mathrm{s}},\sigma_{\mathrm{e}zz}^{\mathrm{s}}=\sigma_{\mathrm{v}zz}^{\mathrm{s}},\phi_{\mathrm{e}}=\phi_{\mathrm{v}},K_{\mathrm{e}}\frac{\partial\phi_{\mathrm{e}}}{\partial z}=K_{\mathrm{v}}\frac{\partial\phi_{\mathrm{v}}}{\partial z} \tag{29}$$

The boundary constraints at the junction between a saturated porous thermoelastic medium and an unsaturated porous thermoelastic media at *z*=*h*1 are as follows:

$$u_{\mathrm{v}zz}^{\mathrm{s}}=u_{\mathrm{u}zz}^{\mathrm{s}},u_{\mathrm{v}xz}^{\mathrm{s}}=u_{\mathrm{u}xz}^{\mathrm{s}},u_{\mathrm{v}zz}^{\mathrm{l}}=u_{\mathrm{u}zz}^{\mathrm{l}},\sigma_{\mathrm{v}zz}^{\mathrm{s}}=\sigma_{\mathrm{u}zz}^{\mathrm{s}},\sigma_{\mathrm{v}xz}^{\mathrm{s}}=\sigma_{\mathrm{u}xz}^{\mathrm{s}},P_{\mathrm{v}}^{\mathrm{l}}=P_{\mathrm{u}}^{\mathrm{l}},P_{\mathrm{u}zz}=0,\phi_{\mathrm{v}}=\phi_{\mathrm{u}},K_{\mathrm{v}}\frac{\partial\phi_{\mathrm{v}}}{\partial z}=K_{\mathrm{u}}\frac{\partial\phi_{\mathrm{u}}}{\partial z} \tag{30}$$

The boundary conditions at the junction between the unsaturated porosity and the free surface at z=0 are as follows:

$$\sigma_{\mathrm{u}zz}^{\mathrm{s}}=0,\sigma_{\mathrm{u}xz}^{\mathrm{s}}=0,P_{\mathrm{u}}^{\mathrm{l}}=0,P_{\mathrm{u}}^{\mathrm{g}}=0,\frac{\partial\phi_{\mathrm{u}}}{\partial z}=0 \tag{31}$$

Expressing stress displacements in the footing

$$\left.\begin{aligned}u_{\mathrm{e}xz}&=\frac{\partial\psi_{\mathrm{e}}^{\mathrm{s}}}{\partial x}-\frac{\partial H_{\mathrm{e}}^{\mathrm{s}}}{\partial z},u_{\mathrm{e}zz}=\frac{\partial\psi_{\mathrm{e}}^{\mathrm{s}}}{\partial z}+\frac{\partial H_{\mathrm{e}}^{\mathrm{s}}}{\partial x},\sigma_{\mathrm{e}xz}=\mu_{\mathrm{e}}(2\frac{\partial^2\psi_{\mathrm{e}}^{\mathrm{s}}}{\partial x\partial z}+\frac{\partial^2H_{\mathrm{e}}^{\mathrm{s}}}{\partial x^2}-\frac{\partial^2H_{\mathrm{e}}^{\mathrm{s}}}{\partial z^2})\\\sigma_{\mathrm{e}zz}&=\lambda_{\mathrm{e}}(\frac{\partial^2\psi_{\mathrm{e}}^{\mathrm{s}}}{\partial x^2}+\frac{\partial^2\psi_{\mathrm{e}}^{\mathrm{s}}}{\partial z^2})+2\mu_{\mathrm{e}}(\frac{\partial^2\psi_{\mathrm{e}}^{\mathrm{s}}}{\partial z^2}+\frac{\partial^2H_{\mathrm{e}}^{\mathrm{s}}}{\partial x\partial z})-3K_{be}\beta_{Te}\phi_{\mathrm{e}}\end{aligned}\right\} \tag{32}$$

Expression of stress and deformation in the saturation layer of the soil

$$\left.\begin{aligned}u_{\mathrm{v}xz}^{\alpha}&=\frac{\partial\psi_{\mathrm{v}}^{\alpha}}{\partial x}-\frac{\partial H_{\mathrm{v}}^{\alpha}}{\partial z},u_{\mathrm{v}zz}^{\alpha}=\frac{\partial\psi_{\mathrm{v}}^{\alpha}}{\partial z}+\frac{\partial H_{\mathrm{v}}^{\alpha}}{\partial x},\sigma_{\mathrm{v}xz}=\mu_{\mathrm{v}}(2\frac{\partial^2\psi_{\mathrm{v}}^{\mathrm{s}}}{\partial x\partial z}+\frac{\partial^2H_{\mathrm{v}}^{\mathrm{s}}}{\partial x^2}-\frac{\partial^2H_{\mathrm{v}}^{\mathrm{s}}}{\partial z^2})\\\sigma_{\mathrm{v}zz}&=2\mu_{\mathrm{v}}(\frac{\partial^2\psi_{\mathrm{v}}^{\mathrm{s}}}{\partial z^2}+\frac{\partial^2H_{\mathrm{v}}^{\mathrm{s}}}{\partial x\partial z})+b_{\mathrm{v}13}\phi_{\mathrm{v}}+b_{\mathrm{v}11}(\frac{\partial^2\psi_{\mathrm{v}}^{\mathrm{s}}}{\partial x^2}+\frac{\partial^2\psi_{\mathrm{v}}^{\mathrm{s}}}{\partial z^2})+b_{\mathrm{v}12}(\frac{\partial^2\psi_{\mathrm{v}}^{\mathrm{l}}}{\partial x^2}+\frac{\partial^2\psi_{\mathrm{v}}^{\mathrm{l}}}{\partial z^2})\\P_{\mathrm{v}}^{\mathrm{l}}&=b_{\mathrm{v}21}(\frac{\partial^2\psi_{\mathrm{v}}^{\mathrm{s}}}{\partial x^2}+\frac{\partial^2\psi_{\mathrm{v}}^{\mathrm{s}}}{\partial z^2})+b_{\mathrm{v}23}\phi_{\mathrm{v}}+b_{\mathrm{v}22}(\frac{\partial^2\psi_{\mathrm{v}}^{\mathrm{l}}}{\partial x^2}+\frac{\partial^2\psi_{\mathrm{v}}^{\mathrm{l}}}{\partial z^2})\end{aligned}\right\} \tag{33}$$

Expression of stress and deformation in the unsaturated soil layer

$$\left.\begin{aligned}
&u_{\mathrm{u}xz}^{\beta}=\frac{\partial\psi_{\mathrm{u}}^{\beta}}{\partial x}-\frac{\partial H_{\mathrm{u}}^{\beta}}{\partial z},\ u_{\mathrm{u}zz}^{\beta}=\frac{\partial\psi_{\mathrm{u}}^{\beta}}{\partial z}+\frac{\partial H_{\mathrm{u}}^{\beta}}{\partial x},\ \sigma_{\mathrm{u}xz}=\mu_{\mathrm{u}}(2\frac{\partial^2\psi_{\mathrm{u}}^{\mathrm{s}}}{\partial x\partial z}+\frac{\partial^2 H_{\mathrm{u}}^{\mathrm{s}}}{\partial x^2}-\frac{\partial^2 H_{\mathrm{u}}^{\mathrm{s}}}{\partial z^2})\\
&\sigma_{\mathrm{u}zz}=\overline{\lambda}_{\mathrm{u}}(\frac{\partial^2\psi_{\mathrm{u}}^{\mathrm{s}}}{\partial x^2}+\frac{\partial^2\psi_{\mathrm{u}}^{\mathrm{s}}}{\partial z^2})+2\mu_{\mathrm{u}}(\frac{\partial^2\psi_{\mathrm{u}}^{\mathrm{s}}}{\partial z^2}+\frac{\partial^2 H_{\mathrm{u}}^{\mathrm{s}}}{\partial x\partial z})+D_1(\frac{\partial^2\psi_{\mathrm{u}}^{\mathrm{l}}}{\partial x^2}+\frac{\partial^2\psi_{\mathrm{u}}^{\mathrm{l}}}{\partial z^2})+D_2(\frac{\partial^2\psi_{\mathrm{u}}^{\mathrm{g}}}{\partial x^2}+\frac{\partial^2\psi_{\mathrm{u}}^{\mathrm{g}}}{\partial z^2})+D_3\phi_{\mathrm{u}}\\
&P_{\mathrm{u}}^{\mathrm{g}}=-B_5(\frac{\partial^2\psi_{\mathrm{u}}^{\mathrm{s}}}{\partial x^2}+\frac{\partial^2\psi_{\mathrm{u}}^{\mathrm{s}}}{\partial z^2})-B_6(\frac{\partial^2\psi_{\mathrm{u}}^{\mathrm{l}}}{\partial x^2}+\frac{\partial^2\psi_{\mathrm{u}}^{\mathrm{l}}}{\partial z^2})-B_7(\frac{\partial^2\psi_{\mathrm{u}}^{\mathrm{g}}}{\partial x^2}+\frac{\partial^2\psi_{\mathrm{u}}^{\mathrm{g}}}{\partial z^2})-B_8\phi_{\mathrm{u}}\\
&P_{\mathrm{u}}^{\mathrm{l}}=-B_1(\frac{\partial^2\psi_{\mathrm{u}}^{\mathrm{s}}}{\partial x^2}+\frac{\partial^2\psi_{\mathrm{u}}^{\mathrm{s}}}{\partial z^2})-B_2(\frac{\partial^2\psi_{\mathrm{u}}^{\mathrm{l}}}{\partial x^2}+\frac{\partial^2\psi_{\mathrm{u}}^{\mathrm{l}}}{\partial z^2})-B_3(\frac{\partial^2\psi_{\mathrm{u}}^{\mathrm{g}}}{\partial x^2}+\frac{\partial^2\psi_{\mathrm{u}}^{\mathrm{g}}}{\partial z^2})-B_4\phi_{\mathrm{u}}
\end{aligned}\right\} \tag{34}$$

Substitution of the wave field function equations (22) - (24) into the boundary condition (31) and the stress displacement expression (34) gives the amplitude coefficients to solve, which can be expressed as the following linear equations:

$$\boldsymbol{F}_{21\times21}\boldsymbol{N}_{21\times1}=A_{\mathrm{is}}\boldsymbol{G}_{21\times1} \tag{35}$$

where $\boldsymbol{N}=[A_{\mathrm{serp1}},A_{\mathrm{serp2}},B_{\mathrm{ers}},A_{\mathrm{svtp1}},A_{\mathrm{svtp2}},A_{\mathrm{svtp3}},A_{\mathrm{svrp1}},A_{\mathrm{svrp2}},A_{\mathrm{svrp3}},B_{\mathrm{svts}},B_{\mathrm{svrs}},$

$A_{\mathrm{sutp1}},A_{\mathrm{sutp2}},A_{\mathrm{sutp3}},A_{\mathrm{sutp4}},A_{\mathrm{surp1}},A_{\mathrm{surp2}},A_{\mathrm{surp3}},A_{\mathrm{surp4}},B_{\mathrm{suts}},B_{\mathrm{surs}}]^{\mathrm{T}}$

$\boldsymbol{F}$ is a 21 × 21 matrix with the elements $f_{1(1)}$ ~ $f_{21(21)}$ and the elements a_1 ~ a_{21} in matrix $\boldsymbol{G}$ given in Appendix B.

3.3 *Displacement of free surface*

The displacement and stress of each point in the site can be determined once the wave field has been determined. Substitute the expressions (22) - (24) into the expressions of the free surface water displacement u_x and the vertical displacement u_z to obtain:

$$\begin{aligned}
u_x=&(A_{\mathrm{surp1}}k_{\mathrm{urp1}}l_{\mathrm{urp1}}+A_{\mathrm{surp2}}k_{\mathrm{urp2}}l_{\mathrm{urp2}}+A_{\mathrm{surp3}}k_{\mathrm{urp3}}l_{\mathrm{urp3}}+A_{\mathrm{surp4}}k_{\mathrm{urp4}}l_{\mathrm{urp4}}+A_{\mathrm{sutp1}}k_{\mathrm{utp1}}l_{\mathrm{utp1}}\\
&+A_{\mathrm{sutp2}}k_{\mathrm{utp2}}l_{\mathrm{utp2}}+A_{\mathrm{sutp3}}k_{\mathrm{utp3}}l_{\mathrm{utp3}}+A_{\mathrm{sutp4}}k_{\mathrm{utp4}}l_{\mathrm{utp4}}-B_{\mathrm{surs}}k_{\mathrm{urs}}n_{\mathrm{urs}}+B_{\mathrm{suts}}k_{\mathrm{uts}}n_{\mathrm{uts}})\mathrm{i};
\end{aligned} \tag{36}$$

$$\begin{aligned}
u_{\mathrm{z}}=&(A_{\mathrm{surp1}}k_{\mathrm{urp1}}n_{\mathrm{urp1}}+A_{\mathrm{surp2}}k_{\mathrm{urp2}}n_{\mathrm{urp2}}+A_{\mathrm{surp3}}k_{\mathrm{urp3}}n_{\mathrm{urp3}}+A_{\mathrm{surp4}}k_{\mathrm{urp4}}n_{\mathrm{urp4}}-A_{\mathrm{sutp1}}k_{\mathrm{utp1}}n_{\mathrm{utp1}}\\
&-A_{\mathrm{sutp2}}k_{\mathrm{utp2}}n_{\mathrm{utp2}}-A_{\mathrm{sutp3}}k_{\mathrm{utp3}}n_{\mathrm{utp3}}-A_{\mathrm{sutp4}}k_{\mathrm{utp4}}n_{\mathrm{utp4}}+B_{\mathrm{surs}}k_{\mathrm{urs}}l_{\mathrm{urs}}+B_{\mathrm{suts}}k_{\mathrm{uts}}l_{\mathrm{uts}})\mathrm{i}
\end{aligned} \tag{37}$$

In this study, the u_x/u_0 and u_z/u_0 amplification factors are used to quantify the horizontal and vertical displacement characteristics at the free-field surface. The amplification factors reflect the displacement amplitude ratio of the site surface in the horizontal and vertical directions relative to the incident wave amplitude, u_0.

4 Numerical examples

4.1 *Verification*

Yang et al. (Yang et al., 2023) investigated the wave motion of a plane S-wave incident from bedrock to unsaturated free site under thermal influence. In verification of the a posteriori solution processes described in this paper, the thickness of the saturated soil h → 0. This degenerates into a problem of seismic ground motion for a plane S-wave incident on a bedrock-unsaturated free-field site under thermal effects. In the verification calculation, physical

parameters consistent with those presented in the aforementioned literature (Yang et al., 2023) are utilized. Figure 2 illustrates that the calculus outcomes of this paper are in substantial alignment with the calculus results of the surface horizontal displacement amplification coefficient in relation to the incident angle in comparison to the literature solutions. This demonstrates the efficacy of the solution methodology presented herein.

The cross-sectional model of the site, depicted in Figure 1, is established to serve as a simulacrum of the bedrock-saturated soil-unsaturated soil site. The lowermost layer of the model is a homogeneous, infinitely deep bedrock stratum, which is considered to be a single-phase elastic medium. The total thickness of the overlying soil is H1 = 100 m, comprising the saturated soil layer with thickness h = 30 m and the unsaturated soil layer with thickness h1 = 70 m. The groundwater level height is denoted by h, while the groundwater depth is defined as (H1-h). By using the displacement amplification factor, this study minimizes potential errors related to soil layer thickness when investigating displacement changes at the free surface.

During the process of seismic wave propagation, it can be identified that the velocity of the S wave is inferior to that of the P wave. In accordance with Snell's Law, the incident angle of the S-wave is lower than the reflected P-wave angle and the transmitted P-wave angle. At this juncture, a critical angle emerges. Should the incident angle of the S-wave exceed the critical angle in question, then the phenomenon of reflection and transmission will cease to exist. The calculation formula $\theta_{cs} = \arcsin(c_{is}/c_{tp})$ of the critical angle indicates that the critical angle is approximately 22°. Accordingly, the range of incident angle variations presented in the subsequent text is defined as 0° to 22°.

Subsequently, the seismic ground motion response of S-wave incident bedrock-saturated soil-unsaturated soil site under thermal effect is studied by numerical calculation, and the influence of physical parameters such as thermal conductivity, saturation and groundwater level on site ground motion is analyzed. The physical parameters used in the numerical calculation are listed in Table 1, Table 2 and Table 3 (Liu 2020a) except for special instructions. The selection of the soil parameters was based on the work of Liu (2020a), and the layer thickness and boundary conditions were referred to the research setting of Hu (2017) to achieve a reasonable simplification of the actual site and reflection of its dynamic characteristics. In this paper, the typical silty sand is taken as the representative, which is widely distributed in natural and engineering environments. It can effectively characterize the thermodynamic behavior of unsaturated soil in the temperature change area, so as to simulate the thermal-hydro-mechanical coupling response of the actual infrastructure site.

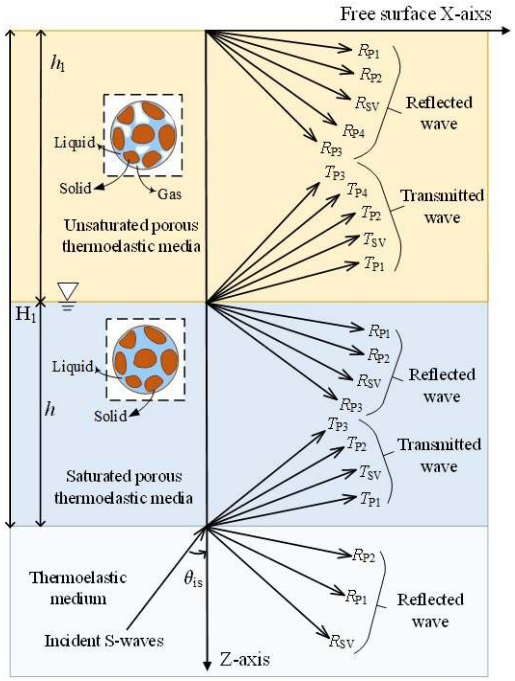

Figure 1. Cross section of bedrock-saturated soil-unsaturated soil site

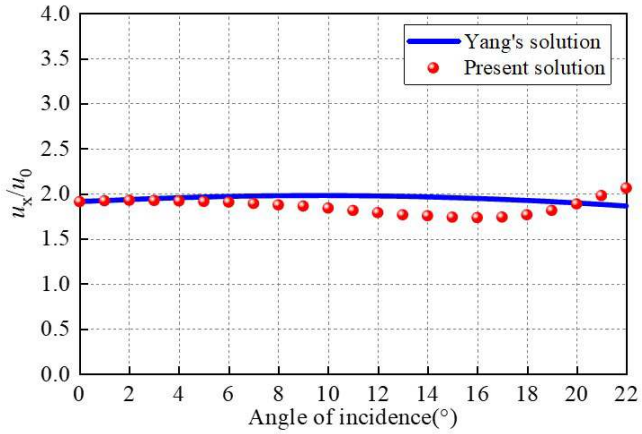

Figure 2. Comparison with Yang et al. (2023) on the variation of the horizontal displacement amplification factor

Table 1. Material parameters for single-phase thermoelastic media (Liu 2020a)

Material parameters	Lame constant	Lame constant	Density	Solid phase heat	Kelvin medium temperature	Initial temperature	Heat flux phase delay time	Frequency
Symbol (unit)	λ_e (KPa)	μ_e (KPa)	ρ_e (kg/m^3)	c_{se} (J/kg/K)	T_e (K)	T_{e0} (K)	τ_{qe} (s)	f (Hz)
Magnitude	12×10^6	8×10^6	2700	1046	293.2	300	2.0×10^{-7}	10

Material parameters	Temperature gradient phase delay time	Thermal expansion coefficient	Coefficient of thermal conductivity
Symbol (unit)	$\tau_{\theta e}$ (s)	β_{Te} (K^{-1})	K_e (J/s/m/K)
Magnitude	1.5×10^{-7}	3.0×10^{-4}	2.5

Table 2. Material parameters of saturated porous thermoelastic media (Liu 2020a)

Material parameters	Lame constant	Lame constant	Porosity	Solid density	Liquid density	Compression modulus of solid particles	Liquid phase compression coefficient
Symbol (unit)	λ_v (KPa)	μ_v (KPa)	n_{vs}	ρ_{vs} (kg/m^3)	ρ_{vl} (kg/m^3)	K_{sv} (KPa)	β_{wpv} (Pa^{-1})
Magnitude	4.4×10^6	2.8×10^6	0.4	2650	1000	3.6×10^7	4.58×10^{-10}

Material parameters	Solid phase thermal expansion coefficient	Coefficient of thermal expansion of liquid phase	Thermal expansion coefficient of saturated porous thermoelastic media	Kelvin medium temperature
Symbol (unit)	β_{sTv} (K^{-1})	β_{wTv} (K^{-1})	β_{Tv} (K^{-1})	T_v (K)
Magnitude	7.8×10^{-6}	2.1×10^{-4}	1.0×10^{-4}	293.2

Material parameters	Initial temperature	Heat flux phase delay time	Temperature gradient phase delay time	Liquid phase specific heat	Solid phase heat	Coefficient of thermal conductivity
Symbol (unit)	T_{v0} (K)	τ_{qv} (s)	$\tau_{\theta v}$ (s)	c_{lv} (J/kg/K)	c_{sv} (J/kg/K)	K_v (J/s/m/K)
Magnitude	300	2.0×10^{-7}	1.5×10^{-7}	4180	1000	2.5

Material parameters	Frequency
Symbol(unit)	f (Hz)
Magnitude	10

Table 3. Material parameters of unsaturated porous thermoelastic media (Liu 2020a)

Material parameters	Lame constant	Lame constant	Porosity	Solid density	Liquid densities	Vapor density	Compression modulus of solid particles	Inherent permeability
Symbol (unit)	λ_{u} (KPa)	μ_{u} (KPa)	n_{us}	ρ_{us} (kg/m^3)	ρ_{ul} (kg/m^3)	ρ_{ug} (kg/m^3)	K_{su} (KPa)	k_{u} (m^2)
Magnitude	4.4×10^{6}	2.8×10^{6}	0.4	2650	1000	1.3	3.6×10^{7}	1×10^{-10}

Material parameters	liquid-phase saturation-degree	Saturation saturation	Residual saturation	Material parameters of V-G model			Solid phase heat	Pore air pressure	Frequency
Symbol (unit)	S_{ul}	$S_{\mathrm{ul}sat}$	$S_{\mathrm{ul}res}$	χ (Pa^{-1})	m	d	c_{su} (J/kg/K)	P_{ug} (KPa)	f (Hz)
Magnitude	0.6	1.0	5%	0.0001	0.5	2	1000	101.3	10

Material parameters	Solid phase thermal expansion coefficient	Coefficient of thermal expansion of liquid phase	Thermal expansion coefficient of porous media	Liquid phase compression coefficient
Symbol (unit)	$\beta_{sT\mathrm{u}}$ (K^{-1})	$\beta_{wT\mathrm{u}}$ (K^{-1})	$\beta_{T\mathrm{u}}$ (K^{-1})	$\beta_{wp\mathrm{u}}$ (Pa^{-1})
Magnitude	7.8×10^{-6}	2.1×10^{-4}	1.0×10^{-4}	4.58×10^{-10}

Material parameters	Heat flux phase delay time	Temperature gradient phase delay time	Coefficient of thermal conductivity	Liquid phase specific heat	Gas compared to heat
Symbol (unit)	$\tau_{q\mathrm{u}}$ (s)	$\tau_{\theta\mathrm{u}}$ (s)	K_{u} (J/s/m/K)	$c_{l\mathrm{u}}$ (J/kg/K)	$c_{g\mathrm{u}}$ (J/kg/K)
Magnitude	2.0×10^{-7}	1.5×10^{-7}	0.4	4180	1900

Material parameters	Kelvin medium temperature	Initial temperature
Symbol (unit)	T_{u} (K)	$T_{\mathrm{u}0}$ (K)
Magnitude	293.2	300

4.2 *Effect of thermal conductivity on free field seismic ground motions under different incident angles*

Thermal conduction is the principal mechanism of heat transfer in the lithosphere. It plays a key role in the exploration of geothermal resources, the detection of high-temperature structures in the lithosphere, and the transmission of seismic waves in high-temperature mediums. Thermal conductance has a wide range of applications (Hou et al., 2021). As shown in Figure 3, before the critical angle is encountered, the vertical and horizontal displacement amplification factors alter with the variation in thermal conductivity. To investigate the influence of thermal conductivity of unsaturated soil on earthquake movement, three values of 0.3J/(m•s•K), 0.4J/(m•s•K) and 0.5J/(m•s•K) were selected to investigate the free field. The values of other related physical quantities are indicated in Table 1, Table 2 and Table 3.

From the evaluation of the values in Figure3, it can be observed that when the S-wave is incidence vertical upward (the angle of incidence is 0°), the vertical dispersion amplification factor of the ground is null, and the horizontal dispersion amplification factor becomes maximum around that moment. With an increasing angle of incidence, the horizontal amplitude amplification coefficient of the site initially declines and then gradually rises, while the vertical amplitude amplification coefficient first grows and then decreases. In particular, Figure 3 illustrates that as the conductivity value increasing, the trend of the displacement enhancement coefficient of the free-field site is coherent, indicating that the variation of the conductivity has a minor impact on the seismic response of the field, which can be almost negligible. Nevertheless, when temperature variations and conditions of steady temperatures are accounted for, the ground motion response of the site exhibits distinct properties. In isothermal elastic wave analysis, the impact of changes in temperature is not considered, causing the elimination of the T-wave in the theoretical model. The consideration of the coupled impact of the variation in temperature is essential when investigating the propagation properties of elastic waves in porous multiphase media, as shown by the divergence of the elastic wave displacement amplification coefficients between isothermal and non-isothermal models. Based on the differences between the propagation coefficients of elastic waves in the isothermal and non-isothermal conditions, it can be inferred that the investigation of the propagation properties of elastic waves in multiphase porous medium is highly relevant to the observation of the coupled phenomenon of temperature variations in the isothermal and non-isothermal conditions.

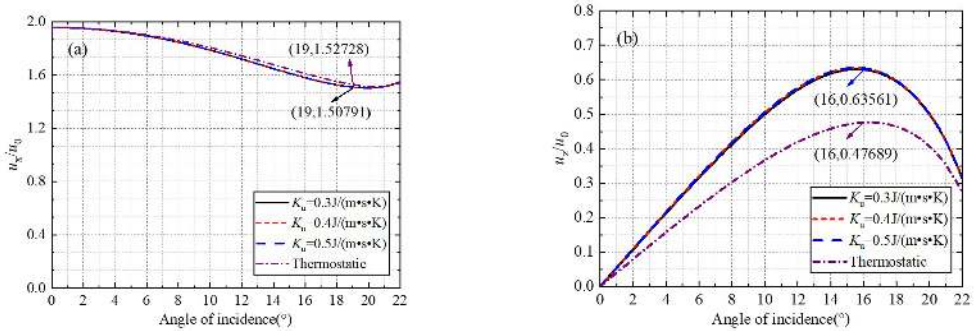

Figure 3. The influence of thermal conductivity on (a) horizontal displacement amplification factor and (b) vertical displacement amplification factor at different incident angles

4.3 *Correlation research between coefficients of thermal expansion and deformation amplification under changing angle of incidence*

The coefficient of heat expansion is a crucial quantity for assessing the thermal expansion of a thermoelastic material. It represents the thermal stability of the media and holds a prominent position in the physics governing the stress-strain relation of bulk materials and heat transfer expression (Hou et al., 2021). Research has demonstrated that the coefficient of thermal expansion has a significant effect on the movement of the site. In this investigation, the variation ranges of thermal dilatation coefficients of unsaturated soil layers are examined, namely 1.0×10-4(K-1) ~ 3.0×10-4(K-1), and the free-field condition is studied. Tables 1, 2 and 3 provide the figures for other relevant physical properties.

Figure 4 shows the variation of the surface displacement amplification coefficient with the thermal expansion coefficient before the critical angle appears. When the S wave is incident vertically at 0°, it mainly produces shear deformation. Since the thermal expansion coefficient is essentially related to the volumetric stress-strain response, and the volumetric strain is negligible under this incident condition, the energy dissipation is minimized, and the seismic wave energy can be efficiently transmitted to the surface. The horizontal displacement amplification factor reaches the maximum (1.468 ~ 1.958), while the vertical displacement amplification factor is zero. With the increase of incident angle, according to Snell 's theorem, S-wave no longer propagates vertically, and wave mode conversion occurs at the interface, resulting in reflection and transmission P-wave, which in turn leads to pore pressure change and energy dissipation, resulting in a gradual decrease in the amplification coefficient of horizontal displacement. At the same time, the P-wave derived from the wave mode conversion increases with the increase of the incident angle, the conversion efficiency gradually increases, and the vertical displacement response increases. However, when the angle exceeds a certain angle, the energy dissipation is significantly enhanced, and the vertical displacement amplification factor gradually decreases. In addition, with the increase of thermal expansion coefficient, the mechanism of thermoelastic coupling and energy dissipation is strengthened, which leads to the increase of vertical displacement amplification coefficient in different degrees within the critical angle range, indicating that the change of thermal expansion coefficient has an important influence on the surface displacement response. It has important reference value for seismic design and seismic risk assessment of engineering sites with significant temperature change areas.

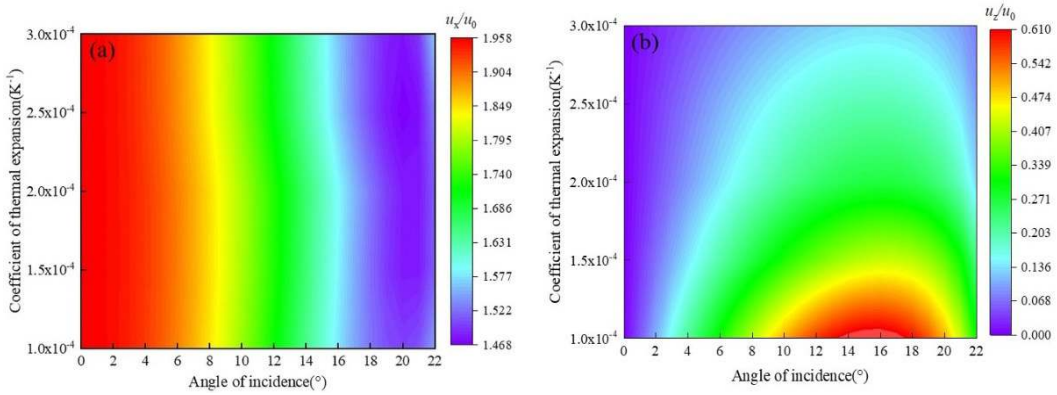

Figure 4. The influence of the coefficient of thermal expansion on (a) the horizontal displacement amplification coefficient and (b) the vertical displacement amplification coefficient under different angles of incidence

4.4 *Observation of the displacement amplification effect of the heat flux phase delay under different incident angles*

A modification of Fourier's law of thermal conductivity is the addition of the phase lag time of the heat flux. It represents the time-lag effect in the process of heat transfer and is used to determine the temporal characteristics in the process of heat conduction. This approach accurately describes non-stationary responses in dynamic heat conduction, thereby establishing a theoretical foundation for heat transfer regulation and optimization in thermodynamic and geotechnical applications. The magnification factors of the vertical and horizontal displacements as a function of the delay time of the heat flow phase up to the appearance of the critical angle are shown in Figure 5. The phase delay time of the heat flux varying from 2.0×10-7(s) to 6.0×10-7(s) and the free field is considered, constraining the scope of the examination to unsaturated soil layers. Other physical parameters are derived from Tables 1, 2 and 3.

Figure 5 demonstrates that at vertical S-wave incidence (incident angle of 0°), the vertical displacement amplification factor vanishes, while the horizontal amplification factor attains its peak. The intrinsic fluctuation band is 1.498 ~ 1.958, which is mostly restricted to the incident angle interval of 0° ~ 8°. In comparison, the vertical displacement amplifying magnitude varied from 0 to 0.654, and its substantial transformation appears in the entrance angle interval of 10° ~ 20°. Meanwhile, as the angle of incidence increases, the amplification factor of the horizontal ground displacement shows a decreasing tendency, while the amplification coefficient of the vertical displacement presents the characteristics of first incrementing and then decrementing. It should be noted that as the phase delay time of the heat flux is increasing, the surface dislocation amplification maintains a steady trend within the marginal angle interval, which is attributed to the solid-liquid-gas three-phase wave formula. The phase delay time of heat flux is not a parameter in the governing equation; therefore, its associated P- and S-wave contributions are negligible. Nevertheless, it can be pointed out that in this situation, only the wave propagation speed of the T-wave is concerned to a specific level, and the wave propagation velocity of the T-wave is generally narrower than that of the P-wave and the S-wave (Liu 2020a). Consequently, for elastic waves incident at any angle, the influence exerted by the variation in heat flux phase delay time on the surface displacement amplification factor remains limited. In view of the low sensitivity of this parameter, it can be reasonably simplified according to the actual situation when constructing the numerical model. It is helpful to avoid the uncertainty caused by the complexity of the model, so as to improve the stability of numerical simulation, the reliability of risk assessment results and the practicality of engineering.

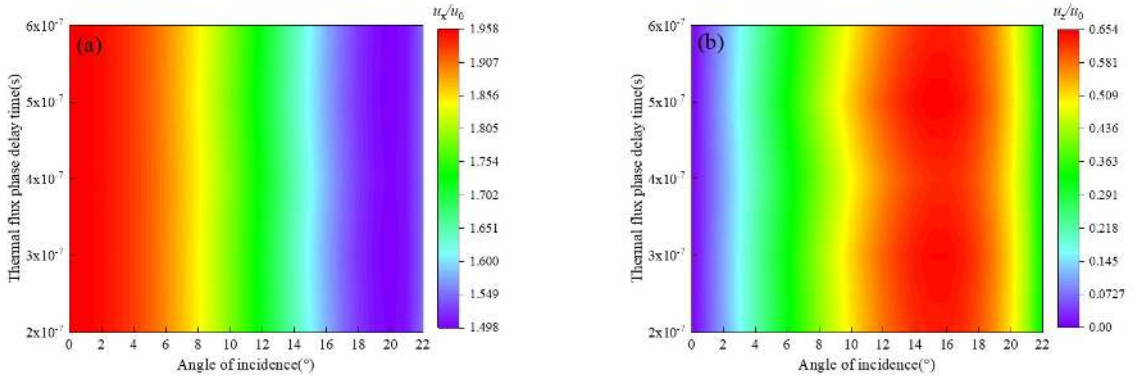

Figure 5. The influence of the coefficient of heat flux phase delay time on (a) the horizontal displacement amplification coefficient and (b) the vertical displacement amplification coefficient under different angles of incidence

4.5 *Quantitative effect of Kelvin medium temperature on displacement amplification at different incident angles*

In seismological research, the dynamic coupling between stress-strain and temperature in crustal bedrock is considered a key factor in the generation and propagation of seismic waves. This coupling directly impacts the physical characteristics of the bedrock, producing a dynamic development of the bedrock physical properties, which decisively determine the sophisticated dynamic features of seismic ground response. Figure 6 illustrates the variation of the amplification coefficients of the vertical and horizontal displacements with the temperature of the Kelvin medium before the occurrence of the critical angle. For the free site, the Kelvin medium temperature of the unsaturated soil layer, namely 273.2(K) ~ 313.2(K), is studied, and other associated property parameters are set according to Table 1, Table 2 and Table 3.

Judging from the observation data presented in Figure 6, when the S-wave is incident vertically upward (the incident angle is 0°), the vertical displacement intensifying factor of the field exhibits the null value, but horizontal displacement increasing coefficient becomes the peak value at this moment. The fluctuating range is 1.50 ~ 1.958, and the principal dynamical fluctuations are clustered in the angle of incidence of 0° ~ 8°. On the opposite, the vertical displacement amplifying factors fluctuate from 0 to 0.680, and its fluctuations are predominantly confined to the angle of incidence of 11° ~ 19°. As the incidence angle progressed, the horizontal displacement enhancement coefficient of the field demonstrated a downward tendency, while the vertical displacement enhancement pattern initially ascended and then descended. It is noteworthy that as the Kelvin medium temperature is elevated, notably at 303.2K, there is an explicit and obvious temperature sensitivity to the vertical displacement gain of the site. From this occurrence it can be inferred that the temperature of the Kelvin medium has a significant effect on the seismic dynamic response.

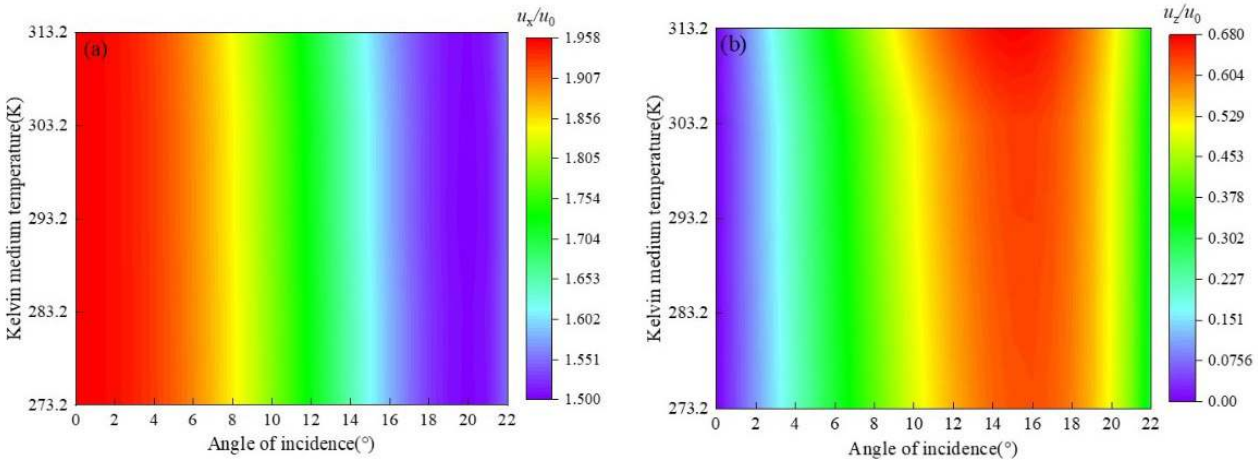

Figure 6. The influence of the coefficient of kelvin medium temperature on (a) the horizontal displacement amplification coefficient and (b) the vertical displacement amplification coefficient under different angles of incidence

4.6 *Response analysis of saturation to surface fluctuation at different incident angles*

In the discipline of soil engineering, the saturation of the layer of soil is normally modified by numerous variables. These variables varying temperature considerably modulates the moisture saturation condition of the site by interfering with the migration movement of the moisture in the soil. Furthermore, some recent investigations have reported (Li et al., 2018) that the changing soil moisture saturation has a considerable contribution to the ground vibration generated by seismic events. As depicted in Figure 7, the vertical and horizontal displacement amplification coefficients of the soil are changed with saturation before the emergence of the critical angle. Assuming that the range of variation of the unsaturated saturation of the soils is 0.4, 0.6 and 0.8, the seismic site analysis is performed. Valuations of other physical characteristics are in Table 1, 2 and 3.

The obtained figures indicate that when the S-wave is incident perpendicularly upwards (the angle of incidence is 0°), the coefficient of amplification of the vertical displacement of the field is null, whereas the coefficient of amplification of the horizontal displacement attains the greatest extent at this instant. As the incident angle increases, the horizontal displacement factor of the site progressively declines, while the vertical displacement gain initially elevates and then declines. As the saturation rises, the horizontal displacement factor progressively declines, while the vertical displacement factor intensifies, and the angle of incidence corresponding to the peak point progressively decreases. It shows that in the heavy rainfall area, the saturation of unsaturated soil layer may change sharply in a short period of time, resulting in the enhancement of vertical displacement amplification effect. Therefore, in the seismic design, the change of soil saturation caused by extreme climate conditions must be fully considered, and the consideration of dynamic response of unsaturated soil must be strengthened, so as to improve the safety and adaptability of the structure under climate disturbance.

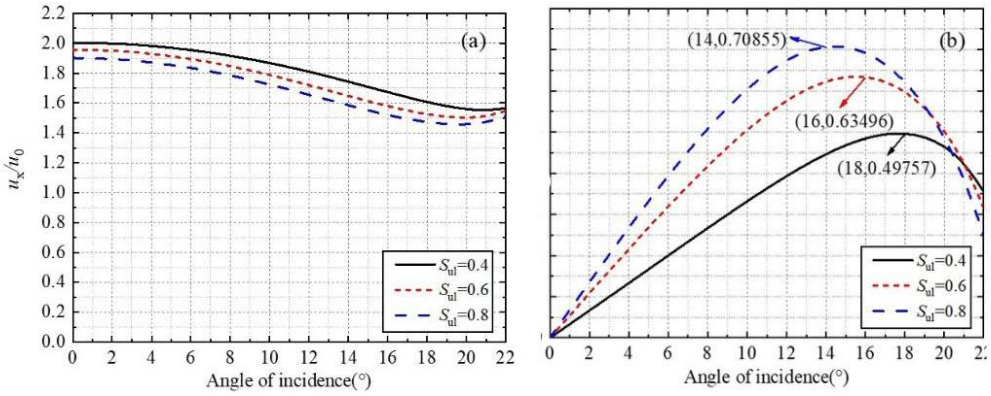

Figure 7. The influence of the saturation degree coefficient on (a) the horizontal displacement amplification coefficient and (b) the vertical displacement amplification coefficient under different angles of incidence

4.7 *Effect of increasing ground water level on free field seismic ground motions at varying incident angles*

As a ubiquitous and activity element in the terrestrial crust, the dynamic variations of groundwater can sensitively represent the signals of seismic and tectonic events. It is noteworthy that the alterations of groundwater level will trigger the modification of soil characteristics in many dimensions, and the impact of seismic wave can lead to the occurrence of the stage transition and slow change phenomenon of groundwater table (Wang et al. 2021), which will have an impact on the generation and transmission of resilient wave. With reference to the investigation reported by Hu (2017), the groundwater level elevation h is assumed to be 0.2H1, 0.3H1 and 0.4H1, respectively, in the numerical analysis to examine the effect of groundwater level fluctuation on the seismic ground movement of the site. The numerical simulation obtained is illustrated in Figure 8, and the figures for the other property parameters are derived from the values shown in Table 1, Table 2 and Table 3, respectively.

By interpreting Figure 8, it can be found that when the S-wave is incident perpendicularly (the incident angle is 0°), the vertical displacement enhancement factor of the field is 0, and the amplification factor for the vertical displacement is not 0. When the groundwater depth is $0.3H_1$ and $0.4H_1$, the displacement amplification factor initially decreases and then increases with the incident angle, with a turning point at 20°. Furthermore, the study indicates that when the groundwater level is 0.3H1 and 0.4H1, the amplification coefficient of horizontal displacement initially declines and then increases with increasing angle of incidence, and the inflection occurs when the angle of incidence exceeds 20°, at which the minimum amplification characteristic of horizontal displacement is achieved. Nevertheless, the horizontal displacement enhancement parameter rises monotonically with the increase of the incident angle when the water table level is 0.2H1. At approximately the equivalent time, the magnification factors of vertical displacement firstly grow and then decline with the increment of the angle of incidence, and the angle of incidence equivalent to the peak value progressively declines. In engineering design, dynamic and refined seismic analysis and design should be carried out according to different groundwater depth in dry season and rainy season, so that the seismic fortification standard of structures can be adjusted accordingly with the change of hydrological conditions.

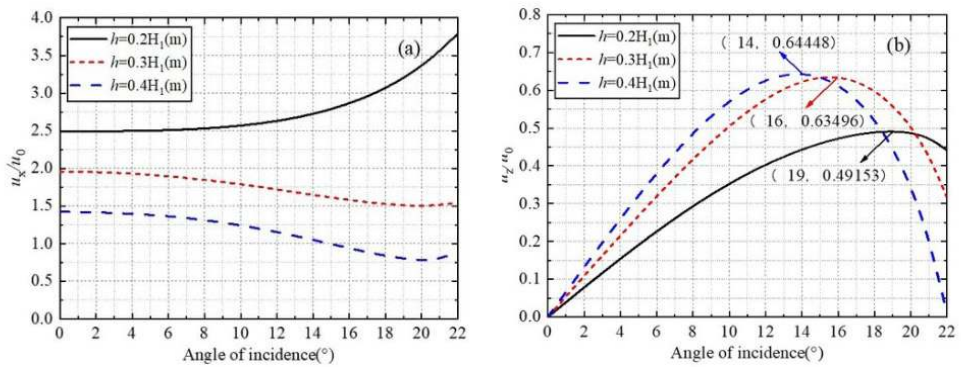

Figure 8. The influence of the coefficient of ground water level on (a) the horizontal displacement amplification coefficient and (b) the vertical displacement amplification coefficient under different angles of incidence

5 Conclusions

In this paper, the numerical analysis of the plane S-wave incident on bedrock-saturated soil-unsaturated soil is performed utilizing the Helmholtz disintegration principle and interface delineations, taking the theory of wave propagation in thermoelastic medium as a basis. Considering the thermal effect as the starting point, the effects of physical parameters such as thermal conductivity, saturation and groundwater level on the displacement amplification factors are comprehensively investigated. The conclusions are as follows:

1. Using the field section model of this paper, numerical simulation analysis shows that the site displacement magnification factors are significantly distinct under thermal influences and isothermal conditions. In particular, the displacement characteristics of the vertical displacement magnification factors under isothermal effects are considerably inferior to those under thermal actions. This demonstrates that temperature variations have an essential effect on the field behavior during the propagation of seismic waves.

2. This paper examines the impact of thermophysical parameters on the propagation characteristics of elastic waves in thermoelastic media. The results of the analysis indicate that as the incident angle is increased, the amplification coefficient of the horizontal displacement of the surface exhibits a decreasing trend, whereas the amplification coefficient of the vertical displacement exhibits a nonlinear change pattern, initially increasing and subsequently decreasing. Further quantitative analysis indicates that the influence of thermal conductivity and phase delay time of heat flux on the amplification coefficient of surface displacement is relatively limited. In contrast, the influence of the thermal expansion coefficient and the Kelvin medium temperature fluctuation on the vertical displacement amplification coefficient is particularly significant. This finding provides a significant theoretical foundation for the intricate dynamic characteristics of elastic wave propagation in thermoelastic media.

3. The characteristics of the soil at a site have a significant influence on the formation and propagation of elastic waves, especially in relation to the role of groundwater level and unsaturated soil saturation in seismic ground movements. By conducting a systematic examination, it was identified that there is a negatively correlated relationship between the amplification coefficient of surface horizontal displacement and groundwater level and saturation. This identification indicates that the amplification coefficient of horizontal displacement gradually decreases with its increase. Conversely, the vertical displacement shows an increasing trend as it increases.

4. In this paper, by exploring the influence of thermal-mechanical coupling on seismic wave propagation in bedrock-saturated soil-unsaturated soil site, it provides theoretical basis and design support for seismic design of major projects, evaluation of high-risk areas of earthquakes and construction of climate-adapted infrastructure. However, when promoting and applying the conclusions of this study, it is necessary to fully consider its applicable boundary: for temperature-sensitive special soil types (such as saline soil, collapsible loess, frozen soil, etc.), due to the significant difference between its permeability and stress-strain relationship and the model in this paper, it is necessary to re-carry out wave theory research or calibrate relevant physical parameters in application; under extreme climatic and hydrological conditions (such as areas strongly affected by tides), the current model needs to be further extended to consider the interaction between dynamic hydrological processes and thermo-mechanical coupling mechanisms; in addition, for high-frequency or ultra-long-period ground motions, the thermal-mechanical coupling response mechanism may be different from the research results in this paper, and specific analysis needs to be carried out separately.

It should be noted that this paper studies the seismic response of bedrock-saturated soil-unsaturated soil site based on the existing elastic theory, but does not take into account the influence of the nonlinear characteristics of the soil on the ground motion response after strong earthquakes. Therefore, there are some limitations in the prediction of the surface seismic response of the site. In this regard, the author will further carry out research on the nonlinear seismic response of the site in the follow-up work.

Acknowledgments

The authors appreciate the Qinghai Province Science and Technology Department Project (No.2024-ZJ-922). The authors are appreciating the helpful suggestions and comments of the reviewers.

Author's Contributions: Conceptualization, Yong-qin Ma and Qiang Ma; Methodology, Yong-qin Ma and Qiang Ma; Investigation, Qiang Ma; Writing - original draft, Yong-qin Ma; Writing - review & editing, Yong-qin Ma and Qiang Ma; Resources, Yong-qin Ma and Qiang Ma; Supervision, Qiang Ma.

Data availability statement: Research data is only available upon request

Editor: Pablo Andrés Muñoz Rojas

Reference

Sánchez-Sesma, F.J., Crouse, C.B. (2015). Effect of site geology on seismic ground motion: early history. Earthq. Eng. Struct. Dyn. 44, 1099–1113.

Trifunac, M.D. (2016). Site conditions and earthquake ground motion – A review. Soil Dyn. Earthq. Eng. 90, 88–100.

Yu, S.S., Zhang, X.Y., Chen, X.C., et al. (2021). Present research situation and prospect on analysis of site seismic response. J. Disaster Prev. Mitig. Eng. 41(1), 181–192.

Wang, L.M., Xu, S.Y., Wang, P., et al. (2024). Characteristics and lessons of liquefaction-triggered large-scale flow slide in loess deposit during Jishishan M6.2 earthquake in 2023. Chin. J. Geotech. Eng. 46(2), 235–243.

Lu, X., Liu, J., Xue, Y., et al. (2023). Analysis of strong earthquake activity characteristics in Taiwan. Acta Seismol. Sin. 45(6), 996–1010.

Ma, Y.J. (2023). Study on thermal property test analysis of shallow rock and soil and heat transfer performance of buried pipe in cold region. Dissertation, Jilin University, China.

Zhang, N., Wang, L., Zhang, Y., et al. (2024). Effect of a V-shaped canyon on the seismic response of a bridge under oblique incident SH waves. Earthq. Eng. Struct. Dyn. 53, 496–514.

Huang, L., Liu, Z.X., Wu, C.Q., et al. (2022). A three-dimensional indirect boundary integral equation method for the scattering of seismic waves in a poroelastic layered half-space. Eng. Anal. Bound. Elem. 135, 167–181.

Ba, Z.N., Liang, J.W. (2017). Fundamental solutions of a multi-layered transversely isotropic saturated half-space subjected to moving point forces and pore pressure. Eng. Anal. Bound. Elem. 76, 40–58.

Ba, Z.N., Wang, Y., Liang, J.W., et al. (2020). Wave scattering of plane P, SV, and SH waves by a 3D alluvial basin in a multilayered half-space. Bull. Seismol. Soc. Am. 110(2), 576–595.

Biot, M.A. (1956). Theory of propagation of elastic wave in fluid saturated porous soil. J. Acoust. Soc. Am. 28(2), 168–178.

Wei, C.F., Muraletharan, K.K. (2002). A continuum theory of porous media saturated by multiple immiscible fluids: I Linear poroelasticity. Int. J. Eng. Sci. 40(16), 1807–1833.

Cai, Y.Q., Li, B.Z., Xu, C.J. (2006). Analysis of elastic wave propagation in sandstone saturated by two immiscible fluids. Chin. J. Rock Mech. Eng. 25(10), 2009–2016.

Xu, M.J., Wei, D.M. (2009). Characteristics of wave propagation in partially saturated poroelastic media. Eng. Sci. Technol. 9(18), 5403–5409.

Ye, C.J., Shi, Y.Y., Cai, Y.Q. (2005). Reflection and refraction at the interface when S waves propagate from saturated soil to elastic soil. J. Vib. Shock 24(2), 41–45+147.

Jiang, L.Z., Guo, Y.R., Chen, Y.H. (2017). Reflection of SV wave at the free surface of saturated soils. China Earthquake Eng. J. 39(6), 1054–1061+1096.

Yang, J. (2001). Saturation effects on horizontal and vertical motions in a layered soil-bedrock system due to inclined SV waves. Soil Dyn. Earthq. Eng. 21(6), 527–536.

Li, W.H. (2002). Influence of water saturation on horizontal and vertical motion at a mainly water-saturated porous soil interface induced by P wave. Rock Soil Mech. 23(6), 782–786.

Li, W.H., Zheng, J., Trifunac, M.D. (2018). Saturation effects on ground motion of unsaturated soil layer-bedrock system excited by plane P and SV waves. Soil Dyn. Earthq. Eng. 110, 159–172.

Xia, T.D., Zhou, X.M. (2006). Propagation characteristics of elastic plane waves in air-saturated soils. J. Jiangnan Univ. 28(6), 711–714+720.

Zhao, H.B., Chen, S.M., Li, L.L., et al. (2012). Influence of fluid saturation on Rayleigh wave propagation. Sci. China Phys. Mech. Astron. 42(2), 148–155.

Chen, W.Y., Xia, T.D., Liu, Z.J., et al. (2013). Reflection of plane S-wave at a free boundary of unsaturated soil. J. Vib. Shock 32(1), 99–103+127.

Yao, T.Q. (2023). Study on the energy characteristics of elastic wave propagation in unsaturated soil. Dissertation, Lanzhou University of Technology, China.

Wang, Y.L., Yuan, X.M., Tong, S.L., et al. (2016). Influence of underground water tables on shear wave velocity of gravelly soils. World Earthq. Eng. 32(3), 72–77.

Hu, Y.C. (2017). Analysis of seismic ground motion of layered unsaturated soil site. Dissertation, Beijing Jiaotong University, China.

Che, J.P. (2018). Time domain algorithm for site response under oblique incident seismic waves. Dissertation, Xi'an University of Technology, China.

Hua, K., Fan, L.M., Chen, J.P. (2019). Characteristics of earthquake ground motion influenced by seismic incident angle. J. Xi'an Univ. Technol. 35(2), 248–255.

Dong, L.D. (2023). Seismic response of a two-layer field under oblique incidence seismic waves. Dissertation, Xi'an University of Technology, China.

Wen, M.J., Wang, K.H., Wu, W.B., et al. (2021). Dynamic response of bilayered saturated porous media based on thermoelastic theory. J. Zhejiang Univ.-Sci. A 22(12), 992–1005.

Li, Y.X. (2023). Study on simulation of seismic wavefield and wave propagation characteristics in thermoacousoelastic medium. Dissertation, Jilin University, China.

Liu, H.B. (2020a). Analysis of propagation characteristics of thermoelastic waves in unsaturated soil. Dissertation, Lanzhou University of Technology, China.

Kaur, I., Singh, K. (2023). Stoneley wave propagation in transversely isotropic thermoelastic rotating medium with memory-dependent derivative and two temperature. Arch. Appl. Mech. 93, 3313–3325.

Yang, Y.Q., Ma, Q. (2024a). Seismic responses of P wave incident stratified unsaturated soil site under thermal effects. Acta Mech. Sin.

Yang, Y.Q., Ma, Q., Zhou, F.X. (2024b). Seismic response study of S-wave incident stratified unsaturated soil site under thermal effects. J. Earthq. Eng. 1–26.

Biot, M. (1956). Thermoelasticity and irreversible thermodynamics. J. Appl. Phys. 27(3), 240–253.

Pecker, C., Deresiewicz, H. (1973). Thermal effects on wave propagation in liquid-filled porous media. Acta Mech. 16(1–2), 45–64.

Berryman, J.G. (1980). Confirmation of Biot's theory. Appl. Phys. Lett. 37(4), 382–384.

Plona, T.J. (1980). Observation of a second bulk compressional wave in a porous medium at ultrasonic frequencies. Appl. Phys. Lett. 36(4), 259–261.

Johnson, D.L., Plona, T.J., Kojima, H. (1994). Probing porous media with first and second sound. II. Acoustic properties of water-saturated porous media. J. Appl. Phys. 76(1), 115–125.

Liu, G.B., Xie, K.H., Zheng, R.Y. (2009). Model of nonlinear coupled thermo-hydro-elastodynamics response for a saturated poroelastic medium. Sci. China Technol. Sci. 52(8), 2372–2383.

Liu, G.B., Zheng, R.Y., Tao, H.B. (2016). Propagation of thermo-elastic wave in saturated porous media. Chin. J. Undergr. Space Eng. 12(4), 926–931.

Zheng, R.Y., Liu, G.B., Deng, Y.B., et al. (2013). Reflection of SV waves at interface of saturated porous thermo-elastic media. Chin. J. Geotech. Eng. 35(S2), 839–843.

Zheng, R.Y., Liu, G.B., Tang, G.J. (2014). Relaxation effects of reflection of SV waves at surface of saturated porous thermoelasticity. J. Natl. Univ. Def. Technol. 36(2), 1–6.

Liu, H.B., Zhou, F.X. (2020b). Propagation characteristics of S-waves in unsaturated soil. China Earthquake Eng. J. 42(4), 960–966.

Liu, H.B., Zhou, F.X., Hao, L.C. (2021). Reflection of plane S waves at the boundary of saturated porous thermo-elastic media. China Earthquake Eng. J. 43(1), 105–112.

Zhou, F.X., Zhang, R.L., Liu, H.B., et al. (2020). Reflection characteristic of plane-S-wave at the free boundary of unsaturated porothermoelastic media. J. Therm. Stress. 43(5), 579–593.

Yang, Y.Q., Ma, Q., Ma, Y.X. (2023). Seismic ground motion study of free-field earthquakes in unsaturated soils incident with SV wave under thermal effects. Eur. Phys. J. Plus 138(10), 927.

Yang, Y.Q., Ma, Q. (2024c). Study on seismic ground motion in the layered elastic ground of S-wave incident under the thermal effect. J. Vib. Eng. Technol. 1–18.

Hou, W.T., Fu, L.Y., Wei, J., et al. (2021). Characteristics of wave propagation in thermoelastic medium. Chin. J. Geophys. 64(4), 1364–1374.

Wang, G.C., Shen, Z.L. (2010). Seismic groundwater monitoring and earthquake prediction. Chin. J. Nat. 32(2), 90–93.

Appendix A. Coefficients *k*e11, *k*e12, *k*e21, *k*e22 in Eq. (4).

$$\left.\begin{aligned}
&k_{\mathrm{e}11}=\rho_{\mathrm{e}}\omega^2-(\lambda_{\mathrm{e}}+2\mu_{\mathrm{e}})k_{\mathrm{pe}}^2\\
&k_{\mathrm{e}12}=-3K_{be}\beta_{T\mathrm{e}}\\
&k_{\mathrm{e}21}=3K_{be}\beta_{T\mathrm{e}}T_{\mathrm{e}0}\left(\mathrm{i}\omega+\tau_{qe}\omega^2\right)k_{\mathrm{pe}}^2\\
&k_{\mathrm{e}22}=K_{\mathrm{e}}\left(1-\tau_{\theta\mathrm{e}}\mathrm{i}\omega\right)k_{\mathrm{pe}}^2-\rho_{\mathrm{e}}c_{s\mathrm{e}}\left(\mathrm{i}\omega+\tau_{qe}\omega^2\right)
\end{aligned}\right\}$$

Coefficients *bvt*11, *bvt*12, *bvt*13, *bvt*21, *bvt*22, *bvt*23, *bvt*31, *bvt*32, *bvt*33, *cvt*11, *cvt*12, *cvt*21, *cvt*22 in Eq. (9). and Eq. (10).

$$\left.\begin{aligned}
&b_{\mathrm{v}t11}=\rho_{\mathrm{v}t}\omega^2-(b_{\mathrm{v}11}+2\mu_{\mathrm{v}})k_{\mathrm{pv}}^2, b_{\mathrm{v}t12}=\rho_{\mathrm{v}l}\omega^2-b_{\mathrm{v}12}k_{\mathrm{pv}}^2\\
&b_{\mathrm{v}t13}=b_{\mathrm{v}13}, b_{\mathrm{v}t21}=\rho_{\mathrm{v}l}\omega^2-b_{\mathrm{v}21}k_{\mathrm{pv}}^2, b_{\mathrm{v}t23}=b_{\mathrm{v}23}, c_{\mathrm{v}t12}=\rho_{\mathrm{v}l}\omega^2\\
&b_{\mathrm{v}t22}=\vartheta_{\mathrm{v}l}\omega^2+\nu_{\mathrm{v}l}\mathrm{i}\omega-b_{\mathrm{v}22}k_{\mathrm{pv}}^2, b_{\mathrm{v}t31}=b_{\mathrm{v}31}(\mathrm{i}\omega+\tau_{q\mathrm{v}}\omega^2)k_{\mathrm{pv}}^2\\
&b_{\mathrm{v}t32}=b_{\mathrm{v}32}(\mathrm{i}\omega+\tau_{q\mathrm{v}}\omega^2)k_{\mathrm{pv}}^2, c_{\mathrm{v}t11}=\rho_{\mathrm{v}l}\omega^2-\mu_{\mathrm{v}}k_{\mathrm{sv}}^2, c_{\mathrm{v}t21}=\rho_{\mathrm{v}l}\omega^2\\
&b_{\mathrm{v}t33}=K_{\mathrm{v}}(1-\tau_{\theta\mathrm{v}}\mathrm{i}\omega)k_{\mathrm{pv}}^2-b_{\mathrm{v}33}(\mathrm{i}\omega+\tau_{q\mathrm{v}}\omega^2), c_{\mathrm{v}t22}=\vartheta_{\mathrm{v}l}\omega^2+\nu_{\mathrm{v}l}\mathrm{i}\omega
\end{aligned}\right\}$$

Coefficients *D*1, *D*2, *D*3, *C*1, *C*2, *C*3, *C*4 in Eq. (11).

$$\left.\begin{aligned}
&D_1=\alpha_{\mathrm{u}}\gamma B_2+\alpha_{\mathrm{u}}(1-\gamma)B_6, D_2=\alpha_{\mathrm{u}}\gamma B_3+\alpha_{\mathrm{u}}(1-\gamma)B_7\\
&D_3=\alpha_{\mathrm{u}}\gamma B_4+\alpha_{\mathrm{u}}(1-\gamma)B_8-\lambda_{\mathrm{u}}^{'}, C_1=\lambda_{\mathrm{u}}^{'}T_{\mathrm{u}0}+\beta_{T\mathrm{u}}T_{\mathrm{u}0}\left[B_1\gamma+B_5(1-\gamma)\right]\\
&C_2=\beta_{T\mathrm{u}}T_{\mathrm{u}0}\left[B_2\gamma+B_6(1-\gamma)\right], C_3=\beta_{T\mathrm{u}}T_{\mathrm{u}0}\left[B_3\gamma+B_7(1-\gamma)\right]\\
&C_4=\tilde{m}+\beta_{T\mathrm{u}}T_{\mathrm{u}0}\left[B_4\gamma+B_8(1-\gamma)\right]
\end{aligned}\right\}$$

Coefficients *d*11*n*, *d*12n, *d*13n, *d*14n, *d*15n, *d*16n, *d*21n, *d*22n, *d*23n, *d*24n, *d*25n, *d*26*n*, *d*31n, *d*32n, *d*33n, *d*34n, *d*35n, *d*36*n* in Eq. (28).

$$\left.\begin{aligned}
&d_{11n}=b_{\mathrm{u}31n}b_{\mathrm{u}43n}-b_{\mathrm{u}41n}b_{\mathrm{u}33n}, d_{12n}=b_{\mathrm{u}11n}b_{\mathrm{u}23n}-b_{\mathrm{u}21n}b_{\mathrm{u}13n}, d_{13n}=b_{\mathrm{u}12n}b_{\mathrm{u}23n}-b_{\mathrm{u}22n}b_{\mathrm{u}13n}\\
&d_{14n}=b_{\mathrm{u}32n}b_{\mathrm{u}43n}-b_{\mathrm{u}42n}b_{\mathrm{u}33n}, d_{15n}=b_{\mathrm{u}14n}b_{\mathrm{u}23n}-b_{\mathrm{u}24n}b_{\mathrm{u}13n}, d_{16n}=b_{\mathrm{u}34n}b_{\mathrm{u}43n}-b_{\mathrm{u}44n}b_{\mathrm{u}33n}\\
&d_{21n}=b_{\mathrm{u}31n}b_{\mathrm{u}42n}-b_{\mathrm{u}41n}b_{\mathrm{u}32n}, d_{22n}=b_{\mathrm{u}11n}b_{\mathrm{u}22n}-b_{\mathrm{u}21n}b_{\mathrm{u}12n}, d_{23n}=b_{\mathrm{u}13n}b_{\mathrm{u}22n}-b_{\mathrm{u}23n}b_{\mathrm{u}12n}\\
&d_{24n}=b_{\mathrm{u}33n}b_{\mathrm{u}42n}-b_{\mathrm{u}43n}b_{\mathrm{u}32n}, d_{25n}=b_{\mathrm{u}14n}b_{\mathrm{u}22n}-b_{\mathrm{u}24n}b_{\mathrm{u}12n}, d_{26n}=b_{\mathrm{u}34n}b_{\mathrm{u}42n}-b_{\mathrm{u}44n}b_{\mathrm{u}32n}\\
&d_{31n}=b_{\mathrm{u}31n}b_{\mathrm{u}43n}-b_{\mathrm{u}41n}b_{\mathrm{u}33n}, d_{32n}=b_{\mathrm{u}11n}b_{\mathrm{u}23n}-b_{\mathrm{u}21n}b_{\mathrm{u}13n}, d_{33n}=b_{\mathrm{u}14n}b_{\mathrm{u}23n}-b_{\mathrm{u}24n}b_{\mathrm{u}13n}\\
&d_{34n}=b_{\mathrm{u}34n}b_{\mathrm{u}43n}-b_{\mathrm{u}44n}b_{\mathrm{u}33n}, d_{35n}=b_{\mathrm{u}12n}b_{\mathrm{u}23n}-b_{\mathrm{u}22n}b_{\mathrm{u}13n}, d_{36n}=b_{\mathrm{u}32n}b_{\mathrm{u}43n}-b_{\mathrm{u}42n}b_{\mathrm{u}33n}
\end{aligned}\right\}$$

Appendix B. The elements $f_{1(1)}$ ~ $f_{21(21)}$ in equation (35) are expressed as follows:

$$f_{1(1)}=k_{\mathrm{erp}1}l_{\mathrm{erp}1}\mathrm{i}\mathrm{e}^{k_{\mathrm{erp}1}n_{\mathrm{erp}1}\mathrm{H}_1\mathrm{i}}; f_{1(2)}=k_{\mathrm{erp}2}l_{\mathrm{erp}2}\mathrm{i}\mathrm{e}^{k_{\mathrm{erp}2}n_{\mathrm{erp}2}\mathrm{H}_1\mathrm{i}}; f_{1(3)}=-k_{\mathrm{ers}}n_{\mathrm{ers}}\mathrm{i}\mathrm{e}^{k_{\mathrm{ers}}n_{\mathrm{ers}}\mathrm{H}_1\mathrm{i}}; f_{1(4)}=-k_{\mathrm{vtp}1}l_{\mathrm{vtp}1}\mathrm{i}e^{-k_{\mathrm{vtp}1}n_{\mathrm{vtp}1}\mathrm{H}_1\mathrm{i}};$$
$$f_{1(5)}=-k_{\mathrm{vtp}2}l_{\mathrm{vtp}2}\mathrm{i}\mathrm{e}^{-k_{\mathrm{vtp}2}n_{\mathrm{vtp}2}\mathrm{H}_1\mathrm{i}}; f_{1(6)}=-k_{\mathrm{vtp}3}l_{\mathrm{vtp}3}\mathrm{i}\mathrm{e}^{-k_{\mathrm{vtp}3}n_{\mathrm{vtp}3}\mathrm{H}_1\mathrm{i}}; f_{1(7)}=-k_{\mathrm{vrp}1}l_{\mathrm{vrp}1}\mathrm{i}\mathrm{e}^{k_{\mathrm{vrp}1}n_{\mathrm{vrp}1}\mathrm{H}_1\mathrm{i}}; f_{1(8)}=-k_{\mathrm{vrp}2}l_{\mathrm{vrp}2}\mathrm{i}\mathrm{e}^{k_{\mathrm{vrp}2}n_{\mathrm{vrp}2}\mathrm{H}_1\mathrm{i}};$$
$$f_{1(9)}=-k_{\mathrm{vrp}3}l_{\mathrm{vrp}3}\mathrm{i}\mathrm{e}^{k_{\mathrm{vrp}3}n_{\mathrm{vrp}3}\mathrm{H}_1\mathrm{i}}; f_{1(12)}=f_{1(13)}=0; f_{1(10)}=-k_{\mathrm{vts}}n_{\mathrm{vts}}\mathrm{i}\mathrm{e}^{-k_{\mathrm{vts}}n_{\mathrm{vts}}\mathrm{H}_1\mathrm{i}}; f_{1(11)}=k_{\mathrm{vrs}}n_{\mathrm{vrs}}\mathrm{i}\mathrm{e}^{k_{\mathrm{vrs}}n_{\mathrm{vrs}}\mathrm{H}_1\mathrm{i}}; f_{1(14)}=f_{1(15)}=0;$$
$$f_{1(16)}=f_{1(17)}=f_{1(18)}=f_{1(19)}=f_{1(20)}=f_{1(21)}=0; f_{2(1)}=k_{\mathrm{erp}1}n_{\mathrm{erp}1}\mathrm{i}\mathrm{e}^{k_{\mathrm{erp}1}n_{\mathrm{erp}1}\mathrm{H}_1\mathrm{i}}; f_{2(2)}=k_{\mathrm{erp}2}n_{\mathrm{erp}2}\mathrm{i}\mathrm{e}^{k_{\mathrm{erp}2}n_{\mathrm{erp}2}\mathrm{H}_1\mathrm{i}}; f_{2(12)}=0;$$

$$f_{2(3)}=k_{\mathrm{ers}}l_{\mathrm{ers}}\mathrm{i}\mathrm{e}^{k_{\mathrm{ers}}n_{\mathrm{ers}}\mathrm{H}_1\mathrm{i}};f_{2(4)}=k_{\mathrm{vtp1}}n_{\mathrm{vtp1}}\mathrm{i}\mathrm{e}^{-k_{\mathrm{vtp1}}n_{\mathrm{vtp1}}\mathrm{H}_1\mathrm{i}};f_{2(5)}=k_{\mathrm{vtp2}}n_{\mathrm{vtp2}}\mathrm{i}\mathrm{e}^{-k_{\mathrm{vtp2}}n_{\mathrm{vtp2}}\mathrm{H}_1\mathrm{i}};f_{2(6)}=k_{\mathrm{vtp3}}n_{\mathrm{vtp3}}\mathrm{i}\mathrm{e}^{-k_{\mathrm{vtp3}}n_{\mathrm{vtp3}}\mathrm{H}_1\mathrm{i}};f_{2(13)}=0;$$
$$f_{2(7)}=-k_{\mathrm{vrp1}}n_{\mathrm{vrp1}}\mathrm{i}\mathrm{e}^{k_{\mathrm{vrp1}}n_{\mathrm{vrp1}}\mathrm{H}_1\mathrm{i}};f_{2(8)}=-k_{\mathrm{vrp2}}n_{\mathrm{vrp2}}\mathrm{i}\mathrm{e}^{k_{\mathrm{vrp2}}n_{\mathrm{vrp2}}\mathrm{H}_1\mathrm{i}};f_{2(9)}=-k_{\mathrm{vrp3}}n_{\mathrm{vrp3}}\mathrm{i}\mathrm{e}^{k_{\mathrm{vrp3}}n_{\mathrm{vrp3}}\mathrm{H}_1\mathrm{i}};f_{2(10)}=-k_{\mathrm{vts}}l_{\mathrm{vts}}\mathrm{i}\mathrm{e}^{-k_{\mathrm{vts}}n_{\mathrm{vts}}\mathrm{H}_1\mathrm{i}};$$
$$f_{2(11)}=-k_{\mathrm{vrs}}l_{\mathrm{vrs}}\mathrm{i}\mathrm{e}^{k_{\mathrm{vrs}}n_{\mathrm{vrs}}\mathrm{H}_1\mathrm{i}};f_{2(14)}=f_{2(15)}=f_{2(16)}=f_{2(17)}=f_{2(18)}=f_{2(19)}=f_{2(20)}=f_{2(21)}=0;\ \ f_{3(1)}=f_{3(2)}=f_{3(3)}=0;$$

$$f_{3(4)}=(\delta_{\mathrm{vlp1}}-1)n_{\mathrm{vtp1}}k_{\mathrm{vtp1}}\mathrm{i}\mathrm{e}^{-k_{\mathrm{vtp1}}n_{\mathrm{vtp1}}\mathrm{H}_1\mathrm{i}};f_{3(5)}=(\delta_{\mathrm{vlp2}}-1)n_{\mathrm{vtp2}}k_{\mathrm{vtp2}}\mathrm{i}\mathrm{e}^{-k_{\mathrm{vtp2}}n_{\mathrm{vtp2}}\mathrm{H}_1\mathrm{i}};f_{3(6)}=(\delta_{\mathrm{vlp3}}-1)n_{\mathrm{vtp3}}k_{\mathrm{vtp3}}\mathrm{i}\mathrm{e}^{-k_{\mathrm{vtp3}}n_{\mathrm{vtp3}}\mathrm{H}_1\mathrm{i}};$$
$$f_{3(7)}=-(\delta_{\mathrm{vlp1}}-1)n_{\mathrm{vrp1}}k_{\mathrm{vrp1}}\mathrm{i}\mathrm{e}^{k_{\mathrm{vrp1}}n_{\mathrm{vrp1}}\mathrm{H}_1\mathrm{i}};f_{3(8)}=-(\delta_{\mathrm{vlp2}}-1)n_{\mathrm{vrp2}}k_{\mathrm{vrp2}}\mathrm{i}\mathrm{e}^{k_{\mathrm{vrp2}}n_{\mathrm{vrp2}}\mathrm{H}_1\mathrm{i}};f_{3(9)}=-(\delta_{\mathrm{vlp3}}-1)n_{\mathrm{vrp3}}k_{\mathrm{vrp3}}\mathrm{i}\mathrm{e}^{k_{\mathrm{vrp3}}n_{\mathrm{vrp3}}\mathrm{H}_1\mathrm{i}};$$
$$f_{3(10)}=-(\delta_{\mathrm{vls}}-1)k_{\mathrm{vts}}l_{\mathrm{vts}}\mathrm{i}\mathrm{e}^{-k_{\mathrm{vts}}n_{\mathrm{vts}}\mathrm{H}_1\mathrm{i}};f_{3(11)}=-(\delta_{\mathrm{vls}}-1)k_{\mathrm{vrs}}l_{\mathrm{vrs}}\mathrm{i}\mathrm{e}^{k_{\mathrm{vrs}}n_{\mathrm{vrs}}\mathrm{H}_1\mathrm{i}};f_{3(12)}=f_{3(13)}=f_{3(14)}=f_{3(15)}=f_{3(16)}=f_{3(17)}=0;$$
$$f_{3(18)}=f_{3(19)}=f_{3(20)}=f_{3(21)}=0;f_{4(1)}=-2\mu_{\mathrm{e}}k_{\mathrm{erp1}}^2l_{\mathrm{erp1}}n_{\mathrm{erp1}}\mathrm{e}^{k_{\mathrm{erp1}}n_{\mathrm{erp1}}\mathrm{H}_1\mathrm{i}};f_{4(2)}=-2\mu_{\mathrm{e}}k_{\mathrm{erp2}}^2l_{\mathrm{erp2}}n_{\mathrm{erp2}}\mathrm{e}^{k_{\mathrm{erp2}}n_{\mathrm{erp2}}\mathrm{H}_1\mathrm{i}};f_{4(12)}=0;$$

$$f_{4(3)}=-\mu_{\mathrm{e}}k_{\mathrm{ers}}^2(l_{\mathrm{ers}}^2-n_{\mathrm{ers}}^2)\mathrm{e}^{k_{\mathrm{ers}}n_{\mathrm{ers}}\mathrm{H}_1\mathrm{i}};f_{4(4)}=-2\mu_{\mathrm{v}}k_{\mathrm{vtp1}}^2l_{\mathrm{vtp1}}n_{\mathrm{vtp1}}e^{-k_{\mathrm{vtp1}}n_{\mathrm{vtp1}}\mathrm{H}_1\mathrm{i}};f_{4(5)}=-2\mu_{\mathrm{v}}k_{\mathrm{vtp2}}^2l_{\mathrm{vtp2}}n_{\mathrm{vtp2}}\mathrm{e}^{-k_{\mathrm{vtp}}n_{\mathrm{vtp2}}\mathrm{H}_1\mathrm{i}};f_{4(13)}=0;$$
$$f_{4(6)}=-2\mu_{\mathrm{v}}k_{\mathrm{vtp3}}^2l_{\mathrm{vtp3}}n_{\mathrm{vtp3}}\mathrm{e}^{-k_{\mathrm{vtp3}}n_{\mathrm{vtp3}}\mathrm{H}_1\mathrm{i}};f_{4(7)}=2\mu_{\mathrm{v}}k_{\mathrm{vrp1}}^2l_{\mathrm{vrp1}}n_{\mathrm{vrp1}}\mathrm{e}^{k_{\mathrm{vrp1}}n_{\mathrm{vrp1}}\mathrm{H}_1\mathrm{i}};f_{4(8)}=2\mu_{\mathrm{v}}k_{\mathrm{vrp2}}^2l_{\mathrm{vrp2}}n_{\mathrm{vrp2}}\mathrm{e}^{k_{\mathrm{vrp2}}n_{\mathrm{vrp2}}\mathrm{H}_1\mathrm{i}};f_{4(14)}=0;$$
$$f_{4(9)}=2\mu_{\mathrm{v}}k_{\mathrm{vrp3}}^2l_{\mathrm{vrp3}}n_{\mathrm{vrp3}}\mathrm{e}^{k_{\mathrm{vrp3}}n_{\mathrm{vrp3}}\mathrm{H}_1\mathrm{i}};f_{4(10)}=\mu_{\mathrm{v}}k_{\mathrm{vts}}^2(l_{\mathrm{vts}}^2-n_{\mathrm{vts}}^2)e^{-k_{\mathrm{vts}}n_{\mathrm{vts}}\mathrm{H}_1\mathrm{i}};f_{4(11)}=\mu_{\mathrm{v}}k_{\mathrm{vrs}}^2(l_{\mathrm{vrs}}^2-n_{\mathrm{vrs}}^2)\mathrm{e}^{k_{\mathrm{vrs}}n_{\mathrm{vrs}}\mathrm{H}_1\mathrm{i}};f_{4(15)}=0;$$

$$f_{5(1)}=-(2\mu_{\mathrm{e}}k_{\mathrm{erp1}}^2n_{\mathrm{erp1}}^2+3\delta_{\mathrm{eTp1}}\beta_{\mathrm{Te}}K_{\mathrm{be}}+\lambda_{\mathrm{e}}k_{\mathrm{erp1}}^2)\mathrm{e}^{k_{\mathrm{erp1}}n_{\mathrm{erp1}}\mathrm{H}_1\mathrm{i}};f_{5(2)}=-(2\mu_{\mathrm{e}}k_{\mathrm{erp2}}^2n_{\mathrm{erp2}}^2+3\delta_{\mathrm{eTp2}}\beta_{\mathrm{Te}}K_{\mathrm{be}}+\lambda_{\mathrm{e}}k_{\mathrm{erp2}}^2)\mathrm{e}^{k_{\mathrm{erp2}}n_{\mathrm{erp2}}\mathrm{H}_1\mathrm{i}};$$
$$f_{5(3)}=-2\mu_{\mathrm{e}}k_{\mathrm{ers}}^2l_{\mathrm{ers}}n_{\mathrm{ers}}\mathrm{e}^{k_{\mathrm{ers}}n_{\mathrm{ers}}\mathrm{H}_1\mathrm{i}};f_{5(4)}=(2\mu_{\mathrm{v}}k_{\mathrm{vtp1}}^2n_{\mathrm{vtp1}}^2+b_{\mathrm{v12}}\delta_{\mathrm{vlp1}}k_{\mathrm{vtp1}}^2+b_{\mathrm{v11}}k_{\mathrm{vtp1}}^2-b_{\mathrm{v13}}\delta_{\mathrm{vTp1}})\mathrm{e}^{-k_{\mathrm{vtp1}}n_{\mathrm{vtp1}}\mathrm{H}_1\mathrm{i}};f_{4(16)}=f_{4(17)}=0;$$
$$f_{5(5)}=(2\mu_{\mathrm{v}}k_{\mathrm{vtp2}}^2n_{\mathrm{vtp2}}^2+b_{\mathrm{v12}}\delta_{\mathrm{vlp2}}k_{\mathrm{vtp2}}^2+b_{\mathrm{v11}}k_{\mathrm{vtp2}}^2-b_{\mathrm{v13}}\delta_{\mathrm{vTp2}})\mathrm{e}^{-k_{\mathrm{vtp2}}n_{\mathrm{vtp2}}\mathrm{H}_1\mathrm{i}};f_{5(10)}=-2\mu_{\mathrm{v}}k_{\mathrm{vts}}^2l_{\mathrm{vts}}n_{\mathrm{vts}}\mathrm{e}^{-k_{\mathrm{vts}}n_{\mathrm{vts}}\mathrm{H}_1\mathrm{i}};f_{4(18)}=0;$$
$$f_{5(7)}=(2\mu_{\mathrm{v}}k_{\mathrm{vrp1}}^2n_{\mathrm{vrp1}}^2+b_{\mathrm{v12}}\delta_{\mathrm{vlp1}}k_{\mathrm{vrp1}}^2+b_{\mathrm{v11}}k_{\mathrm{vrp1}}^2-b_{\mathrm{v13}}\delta_{\mathrm{vTp1}})\mathrm{e}^{k_{\mathrm{vrp1}}n_{\mathrm{vrp1}}\mathrm{H}_1\mathrm{i}};f_{4(19)}=f_{4(20)}=f_{4(21)}=f_{5(12)}=f_{5(13)}=0;$$

$$f_{5(8)}=(2\mu_{\mathrm{v}}k_{\mathrm{vrp2}}^2n_{\mathrm{vrp2}}^2+b_{\mathrm{v12}}\delta_{\mathrm{vlp2}}k_{\mathrm{vrp2}}^2+b_{\mathrm{v11}}k_{\mathrm{vrp2}}^2-b_{\mathrm{v13}}\delta_{\mathrm{vTp2}})\mathrm{e}^{k_{\mathrm{vrp2}}n_{\mathrm{vrp2}}\mathrm{H}_1\mathrm{i}};f_{5(14)}=f_{5(15)}=f_{5(16)}=f_{5(17)}=f_{5(18)}=0;$$

$$f_{5(6)}=(2\mu_{\mathrm{v}}k_{\mathrm{vtp3}}^2n_{\mathrm{vtp3}}^2+b_{\mathrm{v12}}\delta_{\mathrm{vlp3}}k_{\mathrm{vtp3}}^2+b_{\mathrm{v11}}k_{\mathrm{vtp3}}^2-b_{\mathrm{v13}}\delta_{\mathrm{vTp3}})\mathrm{e}^{-k_{\mathrm{vtp3}}n_{\mathrm{vtp3}}\mathrm{H}_1\mathrm{i}};f_{6(1)}=\delta_{\mathrm{eTp1}}\mathrm{e}^{k_{\mathrm{erp1}}n_{\mathrm{erp1}}\mathrm{H}_1\mathrm{i}};f_{6(2)}=\delta_{\mathrm{eTp2}}\mathrm{e}^{k_{\mathrm{erp2}}n_{\mathrm{erp2}}\mathrm{H}_1\mathrm{i}};$$
$$f_{5(9)}=(2\mu_{\mathrm{v}}k_{\mathrm{vrp3}}^2n_{\mathrm{vrp3}}^2+b_{\mathrm{v12}}\delta_{\mathrm{vlp3}}k_{\mathrm{vrp3}}^2+b_{\mathrm{v11}}k_{\mathrm{vrp3}}^2-b_{\mathrm{v13}}\delta_{\mathrm{vTp3}})\mathrm{e}^{k_{\mathrm{vrp3}}n_{\mathrm{vrp3}}\mathrm{H}_1\mathrm{i}};f_{6(4)}=-\delta_{\mathrm{vTp1}}\mathrm{e}^{-k_{\mathrm{vtp1}}n_{\mathrm{vtp1}}\mathrm{H}_1\mathrm{i}};f_{6(5)}=-\delta_{\mathrm{vTp2}}\mathrm{e}^{-k_{\mathrm{vtp2}}n_{\mathrm{vtp2}}\mathrm{H}_1\mathrm{i}};$$
$$f_{6(6)}=-\delta_{\mathrm{vTp3}}\mathrm{e}^{-k_{\mathrm{vtp3}}n_{\mathrm{vtp3}}\mathrm{H}_1\mathrm{i}};f_{6(7)}=-\delta_{\mathrm{vTp1}}\mathrm{e}^{k_{\mathrm{vrp1}}n_{\mathrm{vrp1}}\mathrm{H}_1\mathrm{i}};f_{6(8)}=-\delta_{\mathrm{vTp2}}\mathrm{e}^{k_{\mathrm{vrp2}}n_{\mathrm{vrp2}}\mathrm{H}_1\mathrm{i}};f_{6(9)}=-\delta_{\mathrm{vTp3}}\mathrm{e}^{k_{\mathrm{vrp3}}n_{\mathrm{vrp3}}\mathrm{H}_1\mathrm{i}};f_{5(19)}=f_{5(20)}=0;$$
$$f_{5(21)}=f_{6(3)}=f_{6(10)}=f_{6(11)}=f_{6(12)}=f_{6(13)}=0f_{6(14)}=f_{6(15)}=f_{6(16)}=f_{6(17)}=f_{6(18)}=f_{6(19)}=f_{6(20)}=f_{6(21)}=0;$$

$$f_{7(1)}=\delta_{\mathrm{eTp1}}k_{\mathrm{erp1}}n_{\mathrm{erp1}}K_{\mathrm{e}}\mathrm{i}\mathrm{e}^{k_{\mathrm{erp1}}n_{\mathrm{erp1}}\mathrm{H}_1\mathrm{i}};f_{7(2)}=\delta_{\mathrm{eTp2}}k_{\mathrm{erp2}}n_{\mathrm{erp2}}K_{\mathrm{e}}\mathrm{i}\mathrm{e}^{k_{\mathrm{erp2}}n_{\mathrm{erp2}}\mathrm{H}_1\mathrm{i}};f_{7(3)}=0;f_{7(4)}=\delta_{\mathrm{vTp1}}k_{\mathrm{vtp1}}n_{\mathrm{vtp1}}K_{\mathrm{v}}\mathrm{i}\mathrm{e}^{-k_{\mathrm{vtp1}}n_{\mathrm{vtp1}}\mathrm{H}_1\mathrm{i}};$$

$$f_{7(10)}=f_{7(11)}=0;f_{7(5)}=\delta_{\mathrm{vTp2}}k_{\mathrm{vtp2}}n_{\mathrm{vtp2}}K_{\mathrm{v}}\mathrm{i}\mathrm{e}^{-k_{\mathrm{vtp2}}n_{\mathrm{vtp2}}\mathrm{H}_1\mathrm{i}};f_{7(6)}=\delta_{\mathrm{vTp3}}k_{\mathrm{vtp3}}n_{\mathrm{vtp3}}K_{\mathrm{v}}\mathrm{i}\mathrm{e}^{-k_{\mathrm{vtp3}}\mathrm{n}_{\mathrm{vtp3}}\mathrm{H}_1\mathrm{i}};f_{7(12)}=f_{7(13)}=f_{7(14)}=0;$$
$$f_{7(7)}=-\delta_{\mathrm{vTp1}}k_{\mathrm{vrp1}}n_{\mathrm{vrp1}}K_{\mathrm{v}}\mathrm{i}\mathrm{e}^{k_{\mathrm{vrp1}}n_{\mathrm{vrp1}}\mathrm{H}_1\mathrm{i}};f_{7(8)}=-\delta_{\mathrm{vTp2}}k_{\mathrm{vrp2}}n_{\mathrm{vrp2}}K_{\mathrm{v}}\mathrm{i}\mathrm{e}^{k_{\mathrm{vrp2}}n_{\mathrm{vrp2}}\mathrm{H}_1\mathrm{i}};f_{7(9)}=-\delta_{\mathrm{vTp3}}k_{\mathrm{vrp3}}n_{\mathrm{vrp3}}K_{\mathrm{v}}\mathrm{i}\mathrm{e}^{k_{\mathrm{vrp3}}n_{\mathrm{vrp3}}\mathrm{H}_1\mathrm{i}};$$
$$f_{7(15)}=f_{7(16)}=f_{7(17)}=f_{7(18)}=f_{7(19)}=f_{7(20)}=f_{7(21)}=f_{8(1)}=f_{8(2)}=f_{8(3)}=0;f_{8(4)}=-k_{\mathrm{vtp1}}n_{\mathrm{vtp1}}\mathrm{i}\mathrm{e}^{-k_{\mathrm{vtp1}}n_{\mathrm{vtp1}}h_1\mathrm{i}};$$
$$f_{8(5)}=-k_{\mathrm{vtp2}}n_{\mathrm{vtp2}}\mathrm{i}\mathrm{e}^{-k_{\mathrm{vtp2}}n_{\mathrm{vtp2}}h_1\mathrm{i}};f_{8(6)}=-k_{\mathrm{vtp3}}n_{\mathrm{vtp3}}\mathrm{i}\mathrm{e}^{-k_{\mathrm{vtp3}}n_{\mathrm{vtp3}}h_1\mathrm{i}};f_{8(7)}=k_{\mathrm{vrp1}}n_{\mathrm{vrp1}}\mathrm{i}\mathrm{e}^{k_{\mathrm{vrp1}}n_{\mathrm{vrp1}}h_1\mathrm{i}};f_{8(8)}=k_{\mathrm{vrp2}}n_{\mathrm{vrp2}}\mathrm{i}\mathrm{e}^{k_{\mathrm{vrp2}}n_{\mathrm{vrp2}}h_1\mathrm{i}};$$
$$f_{8(9)}=k_{\mathrm{vrp3}}n_{\mathrm{vrp3}}\mathrm{i}\mathrm{e}^{k_{\mathrm{vrp3}}n_{\mathrm{vrp3}}h_1\mathrm{i}};f_{8(10)}=k_{\mathrm{vts}}l_{\mathrm{vts}}\mathrm{i}\mathrm{e}^{-k_{\mathrm{vts}}n_{\mathrm{vts}}h_1\mathrm{i}};f_{8(11)}=k_{\mathrm{vrs}}l_{\mathrm{vrs}}\mathrm{i}\mathrm{e}^{k_{\mathrm{vrs}}n_{\mathrm{vrs}}h_1\mathrm{i}};f_{8(12)}=k_{\mathrm{utp1}}n_{\mathrm{utp1}}\mathrm{i}\mathrm{e}^{-k_{\mathrm{utp1}}n_{\mathrm{utp1}}h_1\mathrm{i}};$$

$$f_{8(13)}=k_{\mathrm{utp2}}n_{\mathrm{utp2}}\mathrm{i}\mathrm{e}^{-k_{\mathrm{utp2}}n_{\mathrm{utp2}}h_1\mathrm{i}};f_{8(14)}=k_{\mathrm{utp3}}n_{\mathrm{utp3}}\mathrm{i}\mathrm{e}^{-k_{\mathrm{utp3}}n_{\mathrm{utp3}}h_1\mathrm{i}};f_{8(15)}=k_{\mathrm{utp4}}n_{\mathrm{utp4}}\mathrm{i}\mathrm{e}^{-k_{\mathrm{utp4}}\mathrm{n}_{\mathrm{utp4}}h_1\mathrm{i}};f_{8(16)}=-k_{\mathrm{urp1}}n_{\mathrm{urp1}}\mathrm{i}\mathrm{e}^{k_{\mathrm{urp1}}n_{\mathrm{urp1}}h_1\mathrm{i}};$$

$$f_{8(17)}=-k_{\mathrm{urp2}}n_{\mathrm{urp2}}\mathrm{i}\mathrm{e}^{k_{\mathrm{urp2}}n_{\mathrm{urp2}}h_1\mathrm{i}};f_{8(18)}=-k_{\mathrm{urp3}}n_{\mathrm{urp3}}\mathrm{i}\mathrm{e}^{\mathrm{k}_{\mathrm{urp3}}n_{\mathrm{urp3}}h_1\mathrm{i}};f_{8(19)}=-k_{\mathrm{urp4}}n_{\mathrm{urp4}}\mathrm{i}\mathrm{e}^{k_{\mathrm{urp4}}n_{\mathrm{urp4}}h_1\mathrm{i}};f_{8(20)}=-k_{\mathrm{uts}}l_{\mathrm{uts}}\mathrm{i}\mathrm{e}^{-k_{\mathrm{uts}}n_{\mathrm{uts}}h_1\mathrm{i}};$$

$$f_{8(21)}=-k_{\mathrm{urs}}l_{\mathrm{urs}}\mathrm{i}\mathrm{e}^{k_{\mathrm{urs}}n_{\mathrm{urs}}h_1\mathrm{i}};f_{9(1)}=f_{9(2)}=f_{9(3)}=0;f_{9(4)}=k_{\mathrm{vtp1}}l_{\mathrm{vtp1}}\mathrm{i}\mathrm{e}^{-k_{\mathrm{vtp1}}n_{\mathrm{vtp1}}h_1\mathrm{i}};f_{9(5)}=k_{\mathrm{vtp2}}l_{\mathrm{vtp2}}\mathrm{i}\mathrm{e}^{-k_{\mathrm{vtp2}}n_{\mathrm{vtp2}}h_1\mathrm{i}};f_{10(1)}=0;$$
$$f_{9(6)}=k_{\mathrm{vtp3}}l_{\mathrm{vtp3}}\mathrm{i}\mathrm{e}^{-k_{\mathrm{vtp3}}n_{\mathrm{vtp3}}h_1\mathrm{i}};f_{9(7)}=k_{\mathrm{vrp1}}l_{\mathrm{vrp1}}\mathrm{i}e^{k_{\mathrm{vrp1}}n_{\mathrm{vrp1}}h_1\mathrm{i}};f_{9(8)}=k_{\mathrm{vrp2}}l_{\mathrm{vrp2}}\mathrm{i}\mathrm{e}^{k_{\mathrm{vrp2}}n_{\mathrm{vrp2}}h_1\mathrm{i}};f_{9(9)}=k_{\mathrm{vrp3}}l_{\mathrm{vrp3}}\mathrm{i}\mathrm{e}^{k_{\mathrm{vrp3}}n_{\mathrm{vrp3}}h_1\mathrm{i}};f_{10(2)}=0;$$
$$f_{9(10)}=k_{\mathrm{vts}}n_{\mathrm{vts}}\mathrm{i}\mathrm{e}^{-k_{\mathrm{vts}}n_{\mathrm{vts}}h_1\mathrm{i}};f_{9(11)}=-k_{\mathrm{vrs}}n_{\mathrm{vrs}}\mathrm{i}\mathrm{e}^{k_{\mathrm{vrs}}n_{\mathrm{vrs}}h_1\mathrm{i}};f_{9(12)}=-k_{\mathrm{utp1}}l_{\mathrm{utp1}}\mathrm{i}\mathrm{e}^{-k_{\mathrm{utp1}}n_{\mathrm{utp1}}h_1\mathrm{i}};f_{9(13)}=-k_{\mathrm{utp2}}l_{\mathrm{utp2}}\mathrm{i}\mathrm{e}^{-k_{\mathrm{utp2}}n_{\mathrm{utp2}}h_1\mathrm{i}};\quad \mathrm{s}$$
$$f_{9(18)}=-k_{\mathrm{urp3}}l_{\mathrm{urp3}}\mathrm{i}\mathrm{e}^{k_{\mathrm{urp3}}n_{\mathrm{urp3}}h_1\mathrm{i}};f_{9(19)}=-k_{\mathrm{urp4}}l_{\mathrm{urp4}}\mathrm{i}\mathrm{e}^{k_{\mathrm{urp4}}n_{\mathrm{urp4}}h_1\mathrm{i}};f_{9(20)}=-k_{\mathrm{uts}}n_{\mathrm{uts}}\mathrm{i}\mathrm{e}^{-k_{\mathrm{uts}}n_{\mathrm{uts}}h_1\mathrm{i}};f_{9(21)}=k_{\mathrm{urs}}n_{\mathrm{urs}}\mathrm{i}\mathrm{e}^{k_{\mathrm{urs}}n_{\mathrm{urs}}h_1\mathrm{i}};f_{10(3)}=0;$$
$$f_{10(4)}=-\delta_{\mathrm{vlp1}}k_{\mathrm{vtp1}}n_{\mathrm{vtp1}}\mathrm{i}\mathrm{e}^{-k_{\mathrm{vtp1}}n_{\mathrm{vtp1}}h_1\mathrm{i}};f_{10(5)}=-\delta_{\mathrm{vlp2}}k_{\mathrm{vtp2}}n_{\mathrm{vtp2}}\mathrm{i}\mathrm{e}^{-k_{\mathrm{vtp2}}n_{\mathrm{vtp2}}h_1\mathrm{i}};f_{10(6)}=-\delta_{\mathrm{vlp3}}k_{\mathrm{vtp3}}n_{\mathrm{vtp3}}\mathrm{i}\mathrm{e}^{-k_{\mathrm{vtp3}}n_{\mathrm{vtp3}}h_1\mathrm{i}};$$

$$f_{10(7)}=\delta_{\mathrm{vlp1}}k_{\mathrm{vrp1}}n_{\mathrm{vrp1}}\mathrm{i}\mathrm{e}^{k_{\mathrm{vrp1}}n_{\mathrm{vrp1}}h_1\mathrm{i}};f_{10(8)}=\delta_{\mathrm{vlp2}}k_{\mathrm{vrp2}}n_{\mathrm{vrp2}}\mathrm{i}\mathrm{e}^{k_{\mathrm{vrp2}}n_{\mathrm{vrp2}}h_1\mathrm{i}};f_{10(9)}=\delta_{\mathrm{vlp3}}k_{\mathrm{vrp3}}n_{\mathrm{vrp3}}\mathrm{i}\mathrm{e}^{k_{\mathrm{vrp3}}n_{\mathrm{vrp3}}h_1\mathrm{i}};f_{11(1)}=f_{11(2)}=0;$$

$$f_{10(10)}=\delta_{\mathrm{vls}}k_{\mathrm{vts}}l_{\mathrm{vts}}\mathrm{i}\mathrm{e}^{-k_{\mathrm{vts}}n_{\mathrm{vts}}h_1\mathrm{i}};f_{10(11)}=\delta_{\mathrm{vls}}k_{\mathrm{vrs}}l_{\mathrm{vrs}}\mathrm{i}\mathrm{e}^{k_{\mathrm{vrs}}n_{\mathrm{vrs}}h_1\mathrm{i}};f_{10(12)}=\delta_{\mathrm{ulp1}}k_{\mathrm{utp1}}n_{\mathrm{utp1}}\mathrm{i}\mathrm{e}^{-k_{\mathrm{utp1}}n_{\mathrm{utp1}}h_1\mathrm{i}};f_{11(3)}=f_{12(1)}=0;$$

$$f_{10(13)}=\delta_{\mathrm{ulp2}}k_{\mathrm{utp2}}n_{\mathrm{utp2}}\mathrm{i}\mathrm{e}^{-k_{\mathrm{utp2}}n_{\mathrm{utp2}}h_1\mathrm{i}};f_{10(14)}=\delta_{\mathrm{ulp3}}k_{\mathrm{utp3}}n_{\mathrm{utp3}}\mathrm{i}\mathrm{e}^{-k_{\mathrm{utp3}}n_{\mathrm{utp3}}h_1\mathrm{i}};f_{10(15)}=\delta_{\mathrm{ulp4}}k_{\mathrm{utp4}}n_{\mathrm{utp4}}\mathrm{i}\mathrm{e}^{-k_{\mathrm{utp4}}n_{\mathrm{utp4}}h_1\mathrm{i}};f_{12(2)}=0;$$
$$f_{10(16)}=-\delta_{\mathrm{ulp1}}k_{\mathrm{urp1}}n_{\mathrm{urp1}}\mathrm{i}\mathrm{e}^{k_{\mathrm{urp1}}n_{\mathrm{urp1}}h_1\mathrm{i}};f_{10(17)}=-\delta_{\mathrm{ulp2}}k_{\mathrm{urp2}}n_{\mathrm{urp2}}\mathrm{i}\mathrm{e}^{k_{\mathrm{urp2}}n_{\mathrm{urp2}}h_1\mathrm{i}};f_{10(18)}=-\delta_{\mathrm{ulp3}}k_{\mathrm{urp3}}n_{\mathrm{urp3}}\mathrm{i}\mathrm{e}^{k_{\mathrm{urp3}}n_{\mathrm{urp3}}h_1\mathrm{i}};f_{12(3)}=0;$$

$$f_{10(19)}=-\delta_{\mathrm{ulp4}}k_{\mathrm{urp4}}n_{\mathrm{urp4}}\mathrm{i}\mathrm{e}^{k_{\mathrm{urp4}}n_{\mathrm{urp4}}h_1\mathrm{i}};f_{10(20)}=-\delta_{\mathrm{uls}}k_{\mathrm{uts}}l_{\mathrm{uts}}\mathrm{i}\mathrm{e}^{-k_{\mathrm{uts}}n_{\mathrm{uts}}h_1\mathrm{i}};f_{10(21)}=-\delta_{\mathrm{uls}}k_{\mathrm{urs}}l_{\mathrm{urs}}\mathrm{i}\mathrm{e}^{k_{\mathrm{urs}}n_{\mathrm{urs}}h_1\mathrm{i}};f_{13(1)}=f_{13(2)}=0;$$

$$f_{11(4)}=(-2\mu_{\mathrm{v}}k_{\mathrm{vtp1}}^2n_{\mathrm{vtp1}}^2-\delta_{\mathrm{vlp1}}b_{\mathrm{v12}}k_{\mathrm{vtp1}}^2-b_{\mathrm{v11}}k_{\mathrm{vtp1}}^2+b_{\mathrm{v13}}\delta_{\mathrm{vTp1}})\mathrm{e}^{-k_{\mathrm{vtp1}}n_{\mathrm{vtp1}}h_1\mathrm{i}};f_{11(10)}=2\mu_{\mathrm{v}}k_{\mathrm{vts}}^2l_{\mathrm{vts}}n_{\mathrm{vts}}\mathrm{e}^{-k_{\mathrm{vts}}n_{\mathrm{vts}}h_1\mathrm{i}};f_{13(3)}=0;$$
$$f_{11(5)}=(-2\mu_{\mathrm{v}}k_{\mathrm{vtp2}}^2n_{\mathrm{vtp2}}^2-\delta_{\mathrm{vlp2}}b_{\mathrm{v12}}k_{\mathrm{vtp2}}^2-b_{\mathrm{v11}}k_{\mathrm{vtp2}}^2+b_{\mathrm{v13}}\delta_{\mathrm{vTp2}})\mathrm{e}^{-k_{\mathrm{vtp2}}n_{\mathrm{vtp2}}h_1\mathrm{i}};f_{11(11)}=-2\mu_{\mathrm{v}}k_{\mathrm{vrs}}^2l_{\mathrm{vrs}}n_{\mathrm{vrs}}\mathrm{e}^{k_{\mathrm{vrs}}n_{\mathrm{vrs}}h_1\mathrm{i}};f_{13(4)}=0;$$

$$f_{11(6)}=(-2\mu_{\mathrm{v}}k_{\mathrm{vtp3}}^2n_{\mathrm{vtp3}}^2-\delta_{\mathrm{vlp3}}b_{\mathrm{v12}}k_{\mathrm{vtp3}}^2-b_{\mathrm{v11}}k_{\mathrm{vtp3}}^2+b_{\mathrm{v13}}\delta_{\mathrm{vTp3}})\mathrm{e}^{-k_{\mathrm{vtp3}}n_{\mathrm{vtp3}}h_1\mathrm{i}};f_{11(20)}=-2\mu_{\mathrm{u}}k_{\mathrm{uts}}^2l_{\mathrm{uts}}n_{\mathrm{uts}}\mathrm{e}^{-k_{\mathrm{uts}}n_{\mathrm{uts}}h_1\mathrm{i}};f_{13(5)}=0;$$
$$f_{11(7)}=(-2\mu_{\mathrm{v}}k_{\mathrm{vrp1}}^2n_{\mathrm{vrp1}}^2-\delta_{\mathrm{vlp1}}b_{\mathrm{v12}}k_{\mathrm{vrp1}}^2-b_{\mathrm{v11}}k_{\mathrm{vrp1}}^2+b_{\mathrm{v13}}\delta_{\mathrm{vTp1}})\mathrm{e}^{k_{\mathrm{vrp1}}n_{\mathrm{vrp1}}h_1\mathrm{i}};f_{11(21)}=2\mu_{\mathrm{u}}k_{\mathrm{urs}}^2l_{\mathrm{urs}}n_{\mathrm{urs}}\mathrm{e}^{k_{\mathrm{urs}}n_{\mathrm{urs}}h_1\mathrm{i}};f_{13(6)}=0;$$
$$f_{11(8)}=(-2\mu_{\mathrm{v}}k_{\mathrm{vrp2}}^2n_{\mathrm{vrp2}}^2-\delta_{\mathrm{vlp2}}b_{\mathrm{v12}}k_{\mathrm{vrp2}}^2-b_{\mathrm{v11}}k_{\mathrm{vrp2}}^2+b_{\mathrm{v13}}\delta_{\mathrm{vTp2}})\mathrm{e}^{k_{\mathrm{vrp2}}n_{\mathrm{vrp2}}h_1\mathrm{i}};f_{12(4)}=2\mu_{\mathrm{v}}k_{\mathrm{vtp1}}^2l_{\mathrm{vtp1}}n_{\mathrm{vtp1}}\mathrm{e}^{-k_{\mathrm{vtp1}}n_{\mathrm{vtp1}}h_1\mathrm{i}};f_{13(7)}=0;$$

$$f_{11(9)}=(-2\mu_{\mathrm{v}}k_{\mathrm{vrp3}}^2n_{\mathrm{vrp3}}^2-\delta_{\mathrm{vlp3}}b_{\mathrm{v12}}k_{\mathrm{vrp3}}^2-b_{\mathrm{v11}}k_{\mathrm{vrp3}}^2+b_{\mathrm{v13}}\delta_{\mathrm{vTp3}})\mathrm{e}^{k_{\mathrm{vrp3}}n_{\mathrm{vrp3}}h_1\mathrm{i}};f_{12(5)}=2\mu_{\mathrm{v}}k_{\mathrm{vtp2}}^2l_{\mathrm{vtp2}}n_{\mathrm{vtp2}}\mathrm{e}^{-k_{\mathrm{vtp2}}n_{\mathrm{vtp2}}h_1\mathrm{i}};f_{13(8)}=0;$$

$$f_{11(12)}=(2\mu_{\mathrm{u}}k_{\mathrm{utp1}}^2n_{\mathrm{utp1}}^2+\delta_{\mathrm{ulp1}}k_{\mathrm{utp1}}^2D_1+\delta_{\mathrm{ugp1}}k_{\mathrm{utp1}}^2D_2)\mathrm{e}^{-k_{\mathrm{utp1}}n_{\mathrm{utp1}}h_1\mathrm{i}}+(\overline{\lambda}_{\mathrm{u}}k_{\mathrm{utp1}}^2-\delta_{\mathrm{uTp1}}D_3)\mathrm{e}^{-k_{\mathrm{utp1}}n_{\mathrm{utp1}}h_1\mathrm{i}};f_{13(9)}=f_{13(10)}=0;$$

$$f_{11(13)}=(2\mu_{\mathrm{u}}k_{\mathrm{utp2}}^2n_{\mathrm{utp2}}^2+\delta_{\mathrm{ulp2}}k_{\mathrm{utp2}}^2D_1+\delta_{\mathrm{ugp2}}k_{\mathrm{utp2}}^2D_2)\mathrm{e}^{-k_{\mathrm{utp2}}n_{\mathrm{utp2}}h_1\mathrm{i}}+(\overline{\lambda}_{\mathrm{u}}k_{\mathrm{utp2}}^2-\delta_{\mathrm{uTp2}}D_3)\mathrm{e}^{-k_{\mathrm{utp2}}n_{\mathrm{utp2}}h_1\mathrm{i}};f_{13(11)}=f_{13(20)}=0;$$
$$f_{11(14)}=(2\mu_{\mathrm{u}}k_{\mathrm{utp3}}^2n_{\mathrm{utp3}}^2+\delta_{\mathrm{ulp3}}k_{\mathrm{utp3}}^2D_1+\delta_{\mathrm{ugp3}}k_{\mathrm{utp3}}^2D_2)\mathrm{e}^{-k_{\mathrm{utp3}}n_{\mathrm{utp3}}h_1\mathrm{i}}+(\overline{\lambda}_{\mathrm{u}}k_{\mathrm{utp3}}^2-\delta_{\mathrm{uTp3}}D_3)\mathrm{e}^{-k_{\mathrm{utp3}}n_{\mathrm{utp3}}h_1\mathrm{i}};f_{13(21)}=f_{14(1)}=0;$$
$$f_{11(15)}=(2\mu_{\mathrm{u}}k_{\mathrm{utp4}}^2n_{\mathrm{utp4}}^2+\delta_{\mathrm{ulp4}}k_{\mathrm{utp4}}^2D_1+\delta_{\mathrm{ugp4}}k_{\mathrm{utp4}}^2D_2)\mathrm{e}^{-k_{\mathrm{utp4}}n_{\mathrm{utp4}}h_1\mathrm{i}}+(\overline{\lambda}_{\mathrm{u}}k_{\mathrm{utp4}}^2-\delta_{\mathrm{uTp4}}D_3)\mathrm{e}^{-k_{\mathrm{utp4}}n_{\mathrm{utp4}}h_1\mathrm{i}};f_{14(2)}=f_{14(3)}=0;$$
$$f_{11(16)}=(2\mu_{\mathrm{u}}k_{\mathrm{urp1}}^2n_{\mathrm{urp1}}^2+\delta_{\mathrm{ulp1}}k_{\mathrm{urp1}}^2D_1+\delta_{\mathrm{ugp1}}k_{\mathrm{urp1}}^2D_2)\mathrm{e}^{k_{\mathrm{urp1}}n_{\mathrm{urp1}}h_1\mathrm{i}}+(\overline{\lambda}_{\mathrm{u}}k_{\mathrm{urp1}}^2-\delta_{\mathrm{uTp1}}D_3)\mathrm{e}^{k_{\mathrm{urp1}}n_{\mathrm{urp1}}h_1\mathrm{i}};f_{14(10)}=f_{14(11)}=0;$$

$$f_{11(17)}=(2\mu_{\mathrm{u}}k_{\mathrm{urp2}}^2n_{\mathrm{urp2}}^2+\delta_{\mathrm{ulp2}}k_{\mathrm{urp2}}^2D_1+\delta_{\mathrm{ugp2}}k_{\mathrm{urp2}}^2D_2)\mathrm{e}^{k_{\mathrm{urp2}}n_{\mathrm{urp2}}h_1\mathrm{i}}+(\overline{\lambda}_{\mathrm{u}}k_{\mathrm{urp2}}^2-\delta_{\mathrm{uTp2}}D_3)\mathrm{e}^{k_{\mathrm{urp2}}n_{\mathrm{urp2}}h_1\mathrm{i}};f_{14(20)}=f_{14(21)}=0;$$

$$f_{11(18)}=(2\mu_{\mathrm{u}}k_{\mathrm{urp3}}^2n_{\mathrm{urp3}}^2+\delta_{\mathrm{ulp3}}k_{\mathrm{urp3}}^2D_1+\delta_{\mathrm{ugp3}}k_{\mathrm{urp3}}^2D_2)\mathrm{e}^{k_{\mathrm{urp3}}n_{\mathrm{urp3}}h_1\mathrm{i}}+(\overline{\lambda}_{\mathrm{u}}k_{\mathrm{urp3}}^2-\delta_{\mathrm{uTp3}}D_3)\mathrm{e}^{k_{\mathrm{urp3}}n_{\mathrm{urp3}}h_1\mathrm{i}};f_{15(1)}=f_{15(2)}=0;$$

$$f_{11(19)}=(2\mu_{\mathrm{u}}k_{\mathrm{urp4}}^2n_{\mathrm{urp4}}^2+\delta_{\mathrm{ulp4}}k_{\mathrm{urp4}}^2D_1+\delta_{\mathrm{ugp4}}k_{\mathrm{urp4}}^2D_2)\mathrm{e}^{k_{\mathrm{urp4}}n_{\mathrm{urp4}}h_1\mathrm{i}}+(\overline{\lambda}_{\mathrm{u}}k_{\mathrm{urp4}}^2-\delta_{\mathrm{uTp4}}D_3)\mathrm{e}^{k_{\mathrm{urp4}}n_{\mathrm{urp4}}h_1\mathrm{i}};f_{15(3)}=0;$$

$$f_{12(6)}=2\mu_{\mathrm{v}}k_{\mathrm{vtp3}}^2l_{\mathrm{vtp3}}n_{\mathrm{vtp3}}\mathrm{e}^{-k_{\mathrm{vtp3}}n_{\mathrm{vtp3}}h_1\mathrm{i}};f_{12(7)}=-2\mu_{\mathrm{v}}k_{\mathrm{vrp1}}^2l_{\mathrm{vrp1}}n_{\mathrm{vrp1}}\mathrm{e}^{k_{\mathrm{vrp1}}n_{\mathrm{vrp1}}h_1\mathrm{i}};f_{12(8)}=-2\mu_{\mathrm{v}}k_{\mathrm{vrp2}}^2l_{\mathrm{vrp2}}n_{\mathrm{vrp2}}e^{k_{\mathrm{vrp2}}n_{\mathrm{vrp2}}h_1\mathrm{i}};$$

$$f_{12(9)}=-2\mu_{\mathrm{v}}k_{\mathrm{vrp3}}^2l_{\mathrm{vrp3}}n_{\mathrm{vrp3}}\mathrm{e}^{k_{\mathrm{vrp3}}n_{\mathrm{vrp3}}h_1\mathrm{i}};f_{12(10)}=-\mu_{\mathrm{v}}k_{\mathrm{vts}}^2(l_{\mathrm{vts}}^2-n_{\mathrm{vts}}^2)\mathrm{e}^{-k_{\mathrm{vts}}n_{\mathrm{vts}}h_1\mathrm{i}};f_{12(11)}=-\mu_{\mathrm{v}}k_{\mathrm{vrs}}^2(l_{\mathrm{vrs}}^2-n_{\mathrm{vrs}}^2)\mathrm{e}^{k_{\mathrm{vrs}}n_{\mathrm{vrs}}h_1\mathrm{i}};$$

$$f_{12(12)}=-2\mu_{\mathrm{u}}k_{\mathrm{utp1}}^2l_{\mathrm{utp1}}n_{\mathrm{utp1}}\mathrm{e}^{-k_{\mathrm{utp1}}n_{\mathrm{utp1}}h_1\mathrm{i}};f_{12(13)}=-2\mu_{\mathrm{u}}k_{\mathrm{utp2}}^2l_{\mathrm{utp2}}n_{\mathrm{utp2}}\mathrm{e}^{-k_{\mathrm{utp2}}n_{\mathrm{utp2}}h_1\mathrm{i}};f_{12(14)}=-2\mu_{\mathrm{u}}k_{\mathrm{utp3}}^2l_{\mathrm{utp3}}n_{\mathrm{utp3}}\mathrm{e}^{-k_{\mathrm{utp3}}n_{\mathrm{utp3}}h_1\mathrm{i}};$$

$$f_{12(15)}=-2\mu_{\mathrm{u}}k_{\mathrm{utp4}}^2l_{\mathrm{utp4}}n_{\mathrm{utp4}}\mathrm{e}^{-k_{\mathrm{utp4}}n_{\mathrm{utp4}}h_1\mathrm{i}};f_{12(16)}=2\mu_{\mathrm{u}}k_{\mathrm{urp1}}^2l_{\mathrm{urp1}}n_{\mathrm{urp1}}\mathrm{e}^{k_{\mathrm{urp1}}n_{\mathrm{urp1}}h_1\mathrm{i}};f_{12(17)}=2\mu_{\mathrm{u}}k_{\mathrm{urp2}}^2l_{\mathrm{urp2}}n_{\mathrm{urp2}}\mathrm{e}^{k_{\mathrm{urp2}}n_{\mathrm{urp2}}h_1\mathrm{i}};$$

$$f_{12(18)}=2\mu_{\mathrm{u}}k_{\mathrm{urp3}}^2l_{\mathrm{urp3}}n_{\mathrm{urp3}}\mathrm{e}^{k_{\mathrm{urp3}}n_{\mathrm{urp3}}h_1\mathrm{i}};f_{12(19)}=2\mu_{\mathrm{u}}k_{\mathrm{urp4}}^2l_{\mathrm{urp4}}n_{\mathrm{urp4}}\mathrm{e}^{k_{\mathrm{urp4}}n_{\mathrm{urp4}}h_1\mathrm{i}};f_{12(20)}=-\mu_{\mathrm{u}}k_{\mathrm{uts}}^2(n_{\mathrm{uts}}^2-l_{\mathrm{uts}}^2)\mathrm{e}^{-k_{\mathrm{uts}}n_{\mathrm{uts}}h_1\mathrm{i}};$$

$$f_{12(21)}=-\mu_{\mathrm{u}}k_{\mathrm{urs}}^2(n_{\mathrm{urs}}^2-l_{\mathrm{urs}}^2)\mathrm{e}^{k_{\mathrm{urs}}n_{\mathrm{urs}}h_1\mathrm{i}};f_{13(12)}=(\delta_{\mathrm{ulp1}}k_{\mathrm{utp1}}^2B_6+\delta_{\mathrm{ugp1}}k_{\mathrm{utp1}}^2B_7+k_{\mathrm{utp1}}^2B_5-\delta_{\mathrm{uTp1}}B_8)\mathrm{e}^{-k_{\mathrm{utp1}}n_{\mathrm{utp1}}h_1\mathrm{i}};$$

$$f_{13(13)}=(\delta_{\mathrm{ulp2}}k_{\mathrm{utp2}}^2B_6+\delta_{\mathrm{ugp2}}k_{\mathrm{utp2}}^2B_7+k_{\mathrm{utp2}}^2B_5-\delta_{\mathrm{uTp2}}B_8)\mathrm{e}^{-k_{\mathrm{utp2}}n_{\mathrm{utp2}}h_1\mathrm{i}};f_{15(4)}=\delta_{\mathrm{vTp1}}\mathrm{e}^{-k_{\mathrm{vtp1}}n_{\mathrm{vtp1}}h_1\mathrm{i}};f_{15(5)}=\delta_{\mathrm{vTp2}}\mathrm{e}^{-k_{\mathrm{vtp2}}n_{\mathrm{vtp2}}h_1\mathrm{i}};$$

$$f_{13(14)}=(\delta_{\mathrm{ulp3}}k_{\mathrm{utp3}}^2B_6+\delta_{\mathrm{ugp3}}k_{\mathrm{utp3}}^2B_7+k_{\mathrm{utp3}}^2B_5-\delta_{\mathrm{uTp3}}B_8)\mathrm{e}^{-k_{\mathrm{utp3}}n_{\mathrm{utp3}}h_1\mathrm{i}};f_{15(6)}=\delta_{\mathrm{vTp3}}\mathrm{e}^{-k_{\mathrm{vtp3}}n_{\mathrm{vtp3}}h_1\mathrm{i}};f_{15(7)}=\delta_{\mathrm{vTp1}}\mathrm{e}^{k_{\mathrm{vrp1}}n_{\mathrm{vrp1}}h_1\mathrm{i}};$$
$$f_{13(15)}=(\delta_{\mathrm{ulp4}}k_{\mathrm{utp4}}^2B_6+\delta_{\mathrm{ugp4}}k_{\mathrm{utp4}}^2B_7+k_{\mathrm{utp4}}^2B_5-\delta_{\mathrm{uTp4}}B_8)\mathrm{e}^{-k_{\mathrm{utp4}}n_{\mathrm{utp4}}h_1\mathrm{i}};f_{15(8)}=\delta_{\mathrm{vTp2}}\mathrm{e}^{k_{\mathrm{vrp2}}n_{\mathrm{vrp2}}h_1\mathrm{i}};f_{15(9)}=\delta_{\mathrm{vTp3}}\mathrm{e}^{k_{\mathrm{vrp3}}n_{\mathrm{vrp3}}h_1\mathrm{i}};$$

$$f_{13(16)}=(\delta_{\mathrm{ulp1}}k_{\mathrm{urp1}}^2B_6+\delta_{\mathrm{ugp1}}k_{\mathrm{urp1}}^2B_7+k_{\mathrm{urp1}}^2B_5-\delta_{\mathrm{uTp1}}B_8)\mathrm{e}^{k_{\mathrm{urp1}}n_{\mathrm{urp1}}h_1\mathrm{i}};f_{15(12)}=-\delta_{\mathrm{uTp1}}\mathrm{e}^{-k_{\mathrm{utp1}}n_{\mathrm{utp1}}h_1\mathrm{i}};f_{15(13)}=-\delta_{\mathrm{uTp2}}\mathrm{e}^{-k_{\mathrm{utp2}}n_{\mathrm{utp2}}h_1\mathrm{i}};$$
$$f_{13(17)}=(\delta_{\mathrm{ulp2}}k_{\mathrm{urp2}}^2B_6+\delta_{\mathrm{ugp2}}k_{\mathrm{urp2}}^2B_7+k_{\mathrm{urp2}}^2B_5-\delta_{\mathrm{uTp2}}B_8)\mathrm{e}^{k_{\mathrm{urp2}}n_{\mathrm{urp2}}h_1\mathrm{i}};f_{15(14)}=-\delta_{\mathrm{uTp3}}\mathrm{e}^{-k_{\mathrm{utp3}}n_{\mathrm{utp3}}h_1\mathrm{i}};f_{15(15)}=-\delta_{\mathrm{uTp4}}\mathrm{e}^{-k_{\mathrm{utp4}}n_{\mathrm{utp4}}h_1\mathrm{i}};$$

$$f_{13(18)}=(\delta_{\mathrm{ulp3}}k_{\mathrm{urp3}}^2B_6+\delta_{\mathrm{ugp3}}k_{\mathrm{urp3}}^2B_7+k_{\mathrm{urp3}}^2B_5-\delta_{\mathrm{uTp3}}B_8)\mathrm{e}^{k_{\mathrm{urp3}}n_{\mathrm{urp3}}h_1\mathrm{i}};f_{15(16)}=-\delta_{\mathrm{uTp1}}\mathrm{e}^{k_{\mathrm{urp1}}n_{\mathrm{urp1}}h_1\mathrm{i}};f_{15(17)}=-\delta_{\mathrm{uTp2}}\mathrm{e}^{k_{\mathrm{urp2}}n_{\mathrm{urp2}}h_1\mathrm{i}};$$
$$f_{13(19)}=(\delta_{\mathrm{ulp4}}k_{\mathrm{urp4}}^2B_6+\delta_{\mathrm{ugp4}}k_{\mathrm{urp4}}^2B_7+k_{\mathrm{urp4}}^2B_5-\delta_{\mathrm{uTp4}}B_8)\mathrm{e}^{k_{\mathrm{urp4}}n_{\mathrm{urp4}}h_1\mathrm{i}};f_{15(18)}=-\delta_{\mathrm{uTp3}}\mathrm{e}^{k_{\mathrm{urp3}}n_{\mathrm{urp3}}h_1\mathrm{i}};f_{15(19)}=-\delta_{\mathrm{uTp4}}\mathrm{e}^{k_{\mathrm{urp4}}n_{\mathrm{urp4}}h_1\mathrm{i}};$$

$$f_{14(4)}=(b_{\mathrm{v23}}\delta_{\mathrm{vTp1}}-\delta_{\mathrm{vlp1}}b_{\mathrm{v22}}k_{\mathrm{vtp1}}^2-b_{\mathrm{v21}}k_{\mathrm{vtp1}}^2)\mathrm{e}^{-k_{\mathrm{vtp1}}n_{\mathrm{vtp1}}h_1\mathrm{i}};f_{15(10)}=f_{15(11)}=f_{15(20)}=f_{15(21)}=f_{16(1)}=f_{16(2)}=f_{16(3)}=0;$$

$$f_{14(5)}=(b_{\mathrm{v23}}\delta_{\mathrm{vTp2}}-\delta_{\mathrm{vlp2}}b_{\mathrm{v22}}k_{\mathrm{vtp2}}^2-b_{\mathrm{v21}}k_{\mathrm{vtp2}}^2)\mathrm{e}^{-k_{\mathrm{vtp2}}n_{\mathrm{vtp2}}h_1\mathrm{i}};f_{16(4)}=-K_{\mathrm{v}}\delta_{\mathrm{vTp1}}k_{\mathrm{vtp1}}n_{\mathrm{vtp1}}\mathrm{i}\mathrm{e}^{-k_{\mathrm{vtp1}}n_{\mathrm{vtp1}}h_1\mathrm{i}};f_{16(10)}=f_{16(11)}=0;$$

$$f_{14(6)}=(b_{\mathrm{v23}}\delta_{\mathrm{vTp3}}-\delta_{\mathrm{vlp3}}b_{\mathrm{v22}}k_{\mathrm{vtp3}}^2-b_{\mathrm{v21}}k_{\mathrm{vtp3}}^2)\mathrm{e}^{-k_{\mathrm{vtp3}}n_{\mathrm{vtp3}}h_1\mathrm{i}};f_{16(5)}=-K_{\mathrm{v}}\delta_{\mathrm{vTp2}}k_{\mathrm{vtp2}}n_{\mathrm{vtp2}}\mathrm{i}\mathrm{e}^{-k_{\mathrm{vtp2}}n_{\mathrm{vtp2}}h_1\mathrm{i}};f_{16(20)}=f_{16(21)}=0;$$

$$f_{14(7)}=(b_{\mathrm{v23}}\delta_{\mathrm{vTp1}}-\delta_{\mathrm{vlp1}}b_{\mathrm{v22}}k_{\mathrm{vrp1}}^2-b_{\mathrm{v21}}k_{\mathrm{vrp1}}^2)\mathrm{e}^{k_{\mathrm{vrp1}}n_{\mathrm{vrp1}}h_1\mathrm{i}};f_{16(6)}=-K_{\mathrm{v}}\delta_{\mathrm{vTp3}}k_{\mathrm{vtp3}}n_{\mathrm{vtp3}}\mathrm{i}\mathrm{e}^{-k_{\mathrm{vtp3}}n_{\mathrm{vtp3}}h_1\mathrm{i}};f_{17(1)}=f_{17(2)}=0;$$

$$f_{14(8)}=(b_{\mathrm{v23}}\delta_{\mathrm{vTp2}}-\delta_{\mathrm{vlp2}}b_{\mathrm{v22}}k_{\mathrm{vrp2}}^2-b_{\mathrm{v21}}k_{\mathrm{vrp2}}^2)\mathrm{e}^{k_{\mathrm{vrp2}}n_{\mathrm{vrp2}}h_1\mathrm{i}};f_{16(7)}=K_{\mathrm{v}}\delta_{\mathrm{vTp1}}k_{\mathrm{vrp1}}n_{\mathrm{vrp1}}\mathrm{i}\mathrm{e}^{k_{\mathrm{vrp1}}n_{\mathrm{vrp1}}h_1\mathrm{i}};f_{17(3)}=f_{17(4)}=0;$$

$$f_{14(9)}=(b_{\mathrm{v23}}\delta_{\mathrm{vTp3}}-\delta_{\mathrm{vlp3}}b_{\mathrm{v22}}k_{\mathrm{vrp3}}^2-b_{\mathrm{v21}}k_{\mathrm{vrp3}}^2)\mathrm{e}^{k_{\mathrm{vrp3}}n_{\mathrm{vrp3}}h_1\mathrm{i}};f_{16(8)}=K_{\mathrm{v}}\delta_{\mathrm{vTp2}}k_{\mathrm{vrp2}}n_{\mathrm{vrp2}}\mathrm{i}\mathrm{e}^{k_{\mathrm{vrp2}}n_{\mathrm{vrp2}}h_1\mathrm{i}};f_{17(5)}=f_{17(6)}=0;$$

$$f_{14(12)}=(\delta_{\mathrm{uTp1}}B_4-\delta_{\mathrm{ulp1}}k_{\mathrm{utp1}}^2B_2-\delta_{\mathrm{ugp1}}k_{\mathrm{utp1}}^2B_3-k_{\mathrm{utp1}}^2B_1)\mathrm{e}^{-k_{\mathrm{utp1}}n_{\mathrm{utp1}}h_1\mathrm{i}};f_{16(9)}=K_{\mathrm{v}}\delta_{\mathrm{vTp3}}k_{\mathrm{vrp3}}n_{\mathrm{vrp3}}\mathrm{i}\mathrm{e}^{k_{\mathrm{vrp3}}n_{\mathrm{vrp3}}h_1\mathrm{i}};f_{17(7)}=0;$$

$$f_{14(13)}=(\delta_{\mathrm{uTp2}}B_4-\delta_{\mathrm{ulp2}}k_{\mathrm{utp2}}^2B_2-\delta_{\mathrm{ugp2}}k_{\mathrm{utp2}}^2B_3-k_{\mathrm{utp2}}^2B_1)\mathrm{e}^{-k_{\mathrm{utp2}}n_{\mathrm{utp2}}h_1\mathrm{i}};f_{16(12)}=K_{\mathrm{u}}\delta_{\mathrm{uTp1}}k_{\mathrm{utp1}}n_{\mathrm{utp1}}\mathrm{i}\mathrm{e}^{-k_{\mathrm{utp1}}n_{\mathrm{utp1}}h_1\mathrm{i}};f_{17(8)}=0;$$

$$f_{14(14)}=(\delta_{\mathrm{uTp3}}B_4-\delta_{\mathrm{ulp3}}k_{\mathrm{utp3}}^2B_2-\delta_{\mathrm{ugp3}}k_{\mathrm{utp3}}^2B_3-k_{\mathrm{utp3}}^2B_1)\mathrm{e}^{-k_{\mathrm{utp3}}n_{\mathrm{utp3}}h_1\mathrm{i}};f_{16(13)}=K_{\mathrm{u}}\delta_{\mathrm{uTp2}}k_{\mathrm{utp2}}n_{\mathrm{utp2}}\mathrm{i}\mathrm{e}^{-k_{\mathrm{utp2}}n_{\mathrm{utp2}}h_1\mathrm{i}};f_{17(9)}=0;$$

$$f_{14(15)}=(\delta_{\mathrm{uTp4}}B_4-\delta_{\mathrm{ulp4}}k_{\mathrm{utp4}}^2B_2-\delta_{\mathrm{ugp4}}k_{\mathrm{utp4}}^2B_3-k_{\mathrm{utp4}}^2B_1)\mathrm{e}^{-k_{\mathrm{utp4}}n_{\mathrm{utp4}}h_1\mathrm{i}};f_{16(14)}=K_{\mathrm{u}}\delta_{\mathrm{uTp3}}k_{\mathrm{utp3}}n_{\mathrm{utp3}}\mathrm{i}\mathrm{e}^{-k_{\mathrm{utp3}}n_{\mathrm{utp3}}h_1\mathrm{i}};f_{17(10)}=0;$$

$$f_{14(16)}=(\delta_{\mathrm{uTp1}}B_4-\delta_{\mathrm{ulp1}}k_{\mathrm{urp1}}^2B_2-\delta_{\mathrm{ugp1}}k_{\mathrm{urp1}}^2B_3-k_{\mathrm{urp1}}^2B_1)\mathrm{e}^{k_{\mathrm{urp1}}n_{\mathrm{urp1}}h_1\mathrm{i}};f_{16(15)}=K_{\mathrm{u}}\delta_{\mathrm{uTp4}}k_{\mathrm{utp4}}n_{\mathrm{utp4}}\mathrm{i}\mathrm{e}^{-k_{\mathrm{utp4}}n_{\mathrm{utp4}}h_1\mathrm{i}};f_{17(11)}=0;$$

$$f_{14(17)}=(\delta_{\mathrm{uTp2}}B_4-\delta_{\mathrm{ulp2}}k_{\mathrm{urp2}}^2B_2-\delta_{\mathrm{ugp2}}k_{\mathrm{urp2}}^2B_3-k_{\mathrm{urp2}}^2B_1)\mathrm{e}^{k_{\mathrm{urp2}}n_{\mathrm{urp2}}h_1\mathrm{i}};f_{16(16)}=-K_{\mathrm{u}}\delta_{\mathrm{uTp1}}k_{\mathrm{urp1}}n_{\mathrm{urp1}}\mathrm{i}\mathrm{e}^{k_{\mathrm{urp1}}n_{\mathrm{urp1}}h_1\mathrm{i}};f_{18(1)}=0;$$

$$f_{14(18)}=(\delta_{\mathrm{uTp3}}B_4-\delta_{\mathrm{ulp3}}k_{\mathrm{urp3}}^2B_2-\delta_{\mathrm{ugp3}}k_{\mathrm{urp3}}^2B_3-k_{\mathrm{urp3}}^2B_1)\mathrm{e}^{k_{\mathrm{urp3}}n_{\mathrm{urp3}}h_1\mathrm{i}};f_{16(17)}=-K_{\mathrm{u}}\delta_{\mathrm{uTp2}}k_{\mathrm{urp2}}n_{\mathrm{urp2}}\mathrm{i}\mathrm{e}^{k_{\mathrm{urp2}}\mathrm{n}_{\mathrm{urp2}}h_1\mathrm{i}};f_{18(2)}=0;$$

$$f_{14(19)}=(\delta_{\mathrm{uTp4}}B_4-\delta_{\mathrm{ulp4}}k_{\mathrm{urp4}}^2B_2-\delta_{\mathrm{ugp4}}k_{\mathrm{urp4}}^2B_3-k_{\mathrm{urp4}}^2B_1)\mathrm{e}^{k_{\mathrm{urp4}}n_{\mathrm{urp4}}h_1\mathrm{i}};f_{16(18)}=-K_{\mathrm{u}}\delta_{\mathrm{uTp3}}k_{\mathrm{urp3}}n_{\mathrm{urp3}}\mathrm{i}\mathrm{e}^{k_{\mathrm{urp3}}n_{\mathrm{urp3}}h_1\mathrm{i}};f_{18(3)}=0;$$

$$f_{17(12)}=\delta_{\mathrm{uTp1}}D_3-2\mu_{\mathrm{u}}k_{\mathrm{utp1}}^2n_{\mathrm{utp1}}^2-\delta_{\mathrm{ulp1}}D_1k_{\mathrm{utp1}}^2-\delta_{\mathrm{ugp1}}D_2k_{\mathrm{utp1}}^2-\bar{\lambda}_{\mathrm{u}}k_{\mathrm{utp1}}^2;f_{16(19)}=-K_{\mathrm{u}}\delta_{\mathrm{uTp4}}k_{\mathrm{urp4}}n_{\mathrm{urp4}}\mathrm{i}\mathrm{e}^{k_{\mathrm{urp4}}n_{\mathrm{urp4}}h_1\mathrm{i}};$$

$$f_{17(13)}=\delta_{\mathrm{uTp2}}D_3-2\mu_{\mathrm{u}}k_{\mathrm{utp2}}^2n_{\mathrm{utp2}}^2-\delta_{\mathrm{ulp2}}D_1k_{\mathrm{utp2}}^2-\delta_{\mathrm{ugp2}}D_2k_{\mathrm{utp2}}^2-\bar{\lambda}_{\mathrm{u}}k_{\mathrm{utp2}}^2;f_{17(20)}=2\mu_{\mathrm{u}}k_{\mathrm{uts}}^2l_{\mathrm{uts}}n_{\mathrm{uts}};f_{18(4)}=f_{18(5)}=0;$$

$$f_{17(14)}=\delta_{\mathrm{uTp3}}D_3-2\mu_{\mathrm{u}}k_{\mathrm{utp3}}^2n_{\mathrm{utp3}}^2-\delta_{\mathrm{ulp3}}D_1k_{\mathrm{utp3}}^2-\delta_{\mathrm{ugp3}}D_2k_{\mathrm{utp3}}^2-\bar{\lambda}_{\mathrm{u}}k_{\mathrm{utp3}}^2;f_{17(21)}=-2\mu_{\mathrm{u}}k_{\mathrm{urs}}^2l_{\mathrm{urs}}n_{\mathrm{urs}};f_{18(6)}=f_{18(7)}=0;$$

$$f_{17(15)}=\delta_{\mathrm{uTp4}}D_3-2\mu_{\mathrm{u}}k_{\mathrm{utp4}}^2n_{\mathrm{utp4}}^2-\delta_{\mathrm{ulp4}}D_1k_{\mathrm{utp4}}^2-\delta_{\mathrm{ugp4}}D_2k_{\mathrm{utp4}}^2-\bar{\lambda}_{\mathrm{u}}k_{\mathrm{utp4}}^2;f_{18(14)}=2\mu_{\mathrm{u}}k_{\mathrm{utp3}}^2l_{\mathrm{utp3}}n_{\mathrm{utp3}};f_{18(8)}=f_{18(9)}=0;$$

$$f_{17(16)}=\delta_{\mathrm{uTp1}}D_3-2\mu_{\mathrm{u}}k_{\mathrm{urp1}}^2n_{\mathrm{urp1}}^2-\delta_{\mathrm{ulp1}}D_1k_{\mathrm{urp1}}^2-\delta_{\mathrm{ugp1}}D_2k_{\mathrm{urp1}}^2-\bar{\lambda}_{\mathrm{u}}k_{\mathrm{urp1}}^2;f_{18(15)}=2\mu_{\mathrm{u}}k_{\mathrm{utp4}}^2l_{\mathrm{utp4}}n_{\mathrm{utp4}};f_{18(10)}=f_{18(11)}=0;$$

$$f_{17(17)}=\delta_{\mathrm{uTp2}}D_3-2\mu_{\mathrm{u}}k_{\mathrm{urp2}}^2n_{\mathrm{urp2}}^2-\delta_{\mathrm{ulp2}}D_1k_{\mathrm{urp2}}^2-\delta_{\mathrm{ugp2}}D_2k_{\mathrm{urp2}}^2-\bar{\lambda}_{\mathrm{u}}k_{\mathrm{urp2}}^2;f_{18(16)}=-2\mu_{\mathrm{u}}k_{\mathrm{urp1}}^2l_{\mathrm{urp1}}n_{\mathrm{urp1}};f_{19(1)}=f_{19(2)}=0;$$

$$f_{17(18)}=\delta_{\mathrm{uTp3}}D_3-2\mu_{\mathrm{u}}k_{\mathrm{urp3}}^2n_{\mathrm{urp3}}^2-\delta_{\mathrm{ulp3}}D_1k_{\mathrm{urp3}}^2-\delta_{\mathrm{ugp3}}D_2k_{\mathrm{urp3}}^2-\bar{\lambda}_{\mathrm{u}}k_{\mathrm{urp3}}^2;f_{18(17)}=-2\mu_{\mathrm{u}}k_{\mathrm{urp2}}^2l_{\mathrm{urp2}}n_{\mathrm{urp2}};f_{19(3)}=f_{19(4)}=0;$$

$$f_{17(19)}=\delta_{\mathrm{uTp4}}D_3-2\mu_{\mathrm{u}}k_{\mathrm{urp4}}^2n_{\mathrm{urp4}}^2-\delta_{\mathrm{ulp4}}D_1k_{\mathrm{urp4}}^2-\delta_{\mathrm{ugp4}}D_2k_{\mathrm{urp4}}^2-\bar{\lambda}_{\mathrm{u}}k_{\mathrm{urp4}}^2;f_{18(18)}=-2\mu_{\mathrm{u}}k_{\mathrm{urp3}}^2l_{\mathrm{urp3}}n_{\mathrm{urp3}};f_{19(5)}=f_{19(6)}=0;$$

$$f_{18(12)}=2\mu_{\mathrm{u}}k_{\mathrm{utp1}}^2l_{\mathrm{utp1}}n_{\mathrm{utp1}};f_{18(13)}=2\mu_{\mathrm{u}}k_{\mathrm{utp2}}^2l_{\mathrm{utp2}}n_{\mathrm{utp2}};f_{18(19)}=-2\mu_{\mathrm{u}}k_{\mathrm{urp4}}^2l_{\mathrm{urp4}}n_{\mathrm{urp4}};f_{18(20)}=(n_{\mathrm{uts}}^2-l_{\mathrm{uts}}^2)\mu_{\mathrm{u}}k_{\mathrm{uts}}^2;f_{19(7)}=0;$$
$$f_{18(21)}=(n_{\mathrm{urs}}^2-l_{\mathrm{urs}}^2)\mu_{\mathrm{u}}k_{\mathrm{urs}}^2;f_{19(8)}=f_{19(9)}=f_{19(10)}=f_{19(11)}=f_{19(20)}=f_{19(21)}=f_{20(1)}=f_{20(2)}=f_{20(3)}=f_{20(4)}=f_{20(5)}=0;$$
$$f_{19(12)}=B_2\delta_{\mathrm{ulp1}}k_{\mathrm{utp1}}^2+B_3\delta_{\mathrm{ugp1}}k_{\mathrm{utp1}}^2+B_1k_{\mathrm{utp1}}^2-B_4\delta_{\mathrm{uTp1}};f_{19(13)}=B_2\delta_{\mathrm{ulp2}}k_{\mathrm{utp2}}^2+B_3\delta_{\mathrm{ugp2}}k_{\mathrm{utp2}}^2+B_1k_{\mathrm{utp2}}^2-B_4\delta_{\mathrm{uTp2}};$$

$$f_{19(14)}=B_2\delta_{\mathrm{ulp3}}k_{\mathrm{utp3}}^2+B_3\delta_{\mathrm{ugp3}}k_{\mathrm{utp3}}^2+B_1k_{\mathrm{utp3}}^2-B_4\delta_{\mathrm{uTp3}};f_{19(15)}=B_2\delta_{\mathrm{ulp4}}k_{\mathrm{utp4}}^2+B_3\delta_{\mathrm{ugp4}}k_{\mathrm{utp4}}^2+B_1k_{\mathrm{utp4}}^2-B_4\delta_{\mathrm{uTp4}};$$

$$f_{19(16)}=B_2\delta_{\mathrm{ulp1}}k_{\mathrm{urp1}}^2+B_3\delta_{\mathrm{ugp1}}k_{\mathrm{urp1}}^2+B_1k_{\mathrm{urp1}}^2-B_4\delta_{\mathrm{uTp1}};f_{19(17)}=B_2\delta_{\mathrm{ulp2}}k_{\mathrm{urp2}}^2+B_3\delta_{\mathrm{ugp2}}k_{\mathrm{urp2}}^2+B_1k_{\mathrm{urp2}}^2-B_4\delta_{\mathrm{uTp2}};$$

$$f_{19(18)}=B_2\delta_{\mathrm{ulp3}}k_{\mathrm{urp3}}^2+B_3\delta_{\mathrm{ugp3}}k_{\mathrm{urp3}}^2+B_1k_{\mathrm{urp3}}^2-B_4\delta_{\mathrm{uTp3}};f_{19(19)}=B_2\delta_{\mathrm{ulp4}}k_{\mathrm{urp4}}^2+B_3\delta_{\mathrm{ugp4}}k_{\mathrm{urp4}}^2+B_1k_{\mathrm{urp4}}^2-B_4\delta_{\mathrm{uTp4}};$$

$$f_{20(12)} = B_6\delta_{\mathrm{ulp1}}k_{\mathrm{utp1}}^2 + B_7\delta_{\mathrm{ugp1}}k_{\mathrm{utp1}}^2 + B_5k_{\mathrm{utp1}}^2 - B_8\delta_{\mathrm{uTp1}}; f_{20(13)} = B_6\delta_{\mathrm{ulp2}}k_{\mathrm{utp2}}^2 + B_7\delta_{\mathrm{ugp2}}k_{\mathrm{utp2}}^2 + B_5k_{\mathrm{utp2}}^2 - B_8\delta_{\mathrm{uTp2}};$$
$$f_{20(14)} = B_6\delta_{\mathrm{ulp3}}k_{\mathrm{utp3}}^2 + B_7\delta_{\mathrm{ugp3}}k_{\mathrm{utp3}}^2 + B_5k_{\mathrm{utp3}}^2 - B_8\delta_{\mathrm{uTp3}}; f_{20(15)} = B_6\delta_{\mathrm{ulp4}}k_{\mathrm{utp4}}^2 + B_7\delta_{\mathrm{ugp4}}k_{\mathrm{utp4}}^2 + B_5k_{\mathrm{utp4}}^2 - B_8\delta_{\mathrm{uTp4}};$$
$$f_{20(16)} = B_6\delta_{\mathrm{ulp1}}k_{\mathrm{urp1}}^2 + B_7\delta_{\mathrm{ugp1}}k_{\mathrm{urp1}}^2 + B_5k_{\mathrm{urp1}}^2 - B_8\delta_{\mathrm{uTp1}}; f_{20(17)} = B_6\delta_{\mathrm{ulp2}}k_{\mathrm{urp2}}^2 + B_7\delta_{\mathrm{ugp2}}k_{\mathrm{urp2}}^2 + B_5k_{\mathrm{urp2}}^2 - B_8\delta_{\mathrm{uTp2}};$$
$$f_{20(18)} = B_6\delta_{\mathrm{ulp3}}k_{\mathrm{urp3}}^2 + B_7\delta_{\mathrm{ugp3}}k_{\mathrm{urp3}}^2 + B_5k_{\mathrm{urp3}}^2 - B_8\delta_{\mathrm{uTp3}}; f_{20(19)} = B_6\delta_{\mathrm{ulp4}}k_{\mathrm{urp4}}^2 + B_7\delta_{\mathrm{ugp4}}k_{\mathrm{urp4}}^2 + B_5k_{\mathrm{urp4}}^2 - B_8\delta_{\mathrm{uTp4}};$$
$$f_{20(6)} = f_{20(7)} = f_{20(8)} = f_{20(9)} = f_{20(10)} = f_{20(11)} = f_{20(20)} = f_{20(21)} = f_{21(1)} = f_{21(2)} = f_{21(3)} = 0; f_{21(12)} = -\delta_{\mathrm{uTp1}}k_{\mathrm{utp1}}n_{\mathrm{utp1}}\mathrm{i};$$

$$f_{21(13)} = -\delta_{\mathrm{uTp2}}k_{\mathrm{utp2}}n_{\mathrm{utp2}}\mathrm{i}; f_{21(14)} = -\delta_{\mathrm{uTp3}}k_{\mathrm{utp3}}n_{\mathrm{utp3}}\mathrm{i}; f_{21(15)} = -\delta_{\mathrm{uTp4}}k_{\mathrm{utp4}}n_{\mathrm{utp4}}\mathrm{i}; f_{21(16)} = \delta_{\mathrm{uTp1}}k_{\mathrm{urp1}}n_{\mathrm{urp1}}\mathrm{i}; f_{21(4)} = f_{21(5)} = 0;$$

$$f_{21(17)} = \delta_{\mathrm{uTp2}}k_{\mathrm{urp2}}n_{\mathrm{urp2}}\mathrm{i}; f_{21(18)} = \delta_{\mathrm{uTp3}}k_{\mathrm{urp3}}n_{\mathrm{urp3}}\mathrm{i}; f_{21(19)} = \delta_{\mathrm{uTp4}}k_{\mathrm{urp4}}n_{\mathrm{urp4}}\mathrm{i}; f_{21(6)} = f_{21(7)} = f_{21(8)} = f_{21(9)} = 0;$$

$$f_{21(10)} = f_{21(11)} = f_{21(20)} = f_{21(21)} = 0;$$

The elements $g_1 \sim g_{21}$ in equation (35) are expressed as follows:

$$a_1 = -k_{\mathrm{is}}n_{\mathrm{is}}\mathrm{i}\mathrm{e}^{-k_{\mathrm{is}}n_{\mathrm{is}}\mathrm{H}_1\mathrm{i}}; a_2 = -k_{\mathrm{is}}l_{\mathrm{is}}\mathrm{i}\mathrm{e}^{-k_{\mathrm{is}}n_{\mathrm{is}}\mathrm{H}_1\mathrm{i}}; a_3 = 0; a_4 = \mu_{\mathrm{e}}k_{\mathrm{is}}^2(l_{\mathrm{is}}^2 - n_{\mathrm{is}}^2)\mathrm{e}^{-k_{\mathrm{is}}n_{\mathrm{is}}\mathrm{H}_1\mathrm{i}}; a_5 = -2\mu_{\mathrm{e}}l_{\mathrm{is}}n_{\mathrm{is}}k_{\mathrm{is}}^2\mathrm{e}^{-k_{\mathrm{is}}n_{\mathrm{is}}\mathrm{Hi}}; a_6 = a_7 = 0;$$

$$a_8 = a_9 = a_{10} = a_{11} = a_{12} = a_{13} = a_{14} = a_{15} = a_{16} = a_{17} = a_{18} = a_{19} = a_{20} = a_{21} = 0;$$